# Watershed Investment Tool 2.0
# Technical User Guide

**Version I**
**Last Updated 08.27.2020**

This document provides technical details on the Peaks to People Water Fund Watershed Investment Tool.

Author: Ben Gannon, Research Associate, Colorado Forest Restoration Institute, Colorado State University
Email: benjamin.gannon@colostate.edu


Science and technical contributors:
Yu Wei, Forest and Rangeland Stewardship, Colorado State University
Lee H. MacDonald, Ecosystem Science and Sustainability, Colorado State University
Stephanie K. Kampf, Ecosystem Science and Sustainability, Colorado State University
Kelly W. Jones, Human Dimensions of Natural Resources, Colorado State University
Jeffery B. Cannon, formerly Colorado Forest Restoration Institute, Colorado State University
Brett H. Wolk, Colorado Forest Restoration Institute, Colorado State University
Antony S. Cheng, Colorado Forest Restoration Institute, Colorado State University
Robert N. Addington, The Nature Conservancy

## Table of Contents

## Introduction

The Watershed Investment Tool (WIT) is a modular wildfire risk assessment and fuels reduction prioritization system designed for the Peaks to People Water Fund (hereafter Peaks to People). The core functions are aimed at quantifying wildfire risk to water supplies and prioritizing the locations and type of fuels reduction treatments to minimize risk. It also includes assessment workflows to calculate performance metrics on the modeled benefits of past and planned fuel treatments. The modeled performance metrics include several co-benefits of fuels reduction for source water protection like risk mitigation to structures in the wildland urban interface, critical wildlife habitat, and recreational assets, among others. The combined capabilities allow for program-level prioritization of fuels reduction work across large watersheds, accounting of implemented project accomplishments, and evaluating the potential benefits of proposed projects. Several of the intermediate spatial and tabular products also have utility for project-level planning.

The core water supply and co-benefits risk assessments that underly the WIT are rooted in established methods for wildfire risk assessment (Finney 2005; Scott et al. 2013) that conceive of risk as the product of fire likelihood and fire consequences. Fire consequences are quantified in this framework using a combination of fire modeling to characterize the intensity of disturbance with an effects assessment to translate fire intensity into ecological, social, or economic net value change. Quantifying risk therefore requires modeling to characterize fire likelihood, fire behavior, and effects, which form the wildfire risk triangle (Figure 1). Details on data sources and modeling methods used in our assessments are provided later in the user guide.

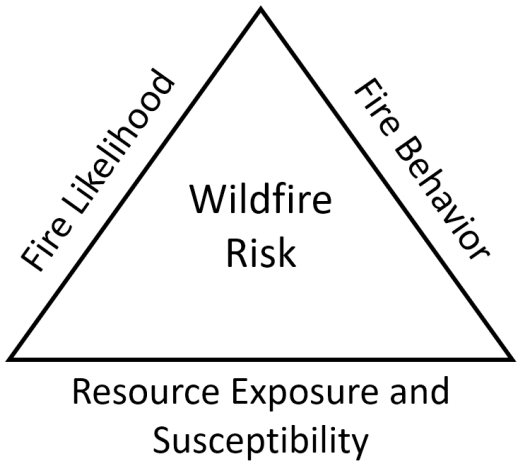


*Figure 1: Wildfire risk triangle adapted from Scott et al. (2013).*

Throughout the user guide and associated WIT products, we make use of the terms *conditional* and *expected* net value change. Expected Net Value Change (eNVC) is a whole actuarial measure of risk incorporating the probability of fire occurrence. Conditional Net Value Change (cNVC) refers to the predicted change in value conditional on (or *given*) fire

occurrence. We highlight both conditional and expected metrics in the WIT because there are some locations on the landscape where models suggest fire likelihood is low, but consequences are high. These measures should be considered in tandem to understand the relative contributions of likelihood and consequences to risk.

*Unique benefits of the WIT*

Wildfire risk assessments often account for wildfire risk to multiple *highly valued resources and assets* (HVRAs) using relative measures of effects on a scale from -100 for total loss to +100 for radical gain (Scott et al. 2013). Consistently valuing effects on a relative scale facilitates combining the resulting measures of risk for each HVRA into a composite measure of total risk based on management priorities or social values (Scott et al. 2013). This approach is well-suited for the style of multi-resource management used by public agencies, but a downside of this approach is that relativized measures of risk do not clearly communicate risk in absolute terms such as the expected sediment delivery to a reservoir and associated costs. Peaks to People sought for the WIT to measure risk in monetary terms, as much as possible, to foster the view that proactive mitigation in watershed management is a financial investment with transparent benefits and costs. The WIT takes a detailed approach to quantifying wildfire risk to water supplies in monetary terms motivated by earlier efforts in California (Buckley et al. 2014; Elliot et al. 2016). Where possible, the co-benefits of source water mitigation measures are also valued in dollars.

Use of wildfire risk assessments in land and watershed management is now commonplace, but it is rare that these assessments go beyond characterizing baseline conditions to plan efficient mitigation programs with analysis of fuel treatment effectiveness, opportunities, and costs. Risk mitigation is quantified in the WIT by modeling the primary effects of fuel treatments on the input fuels data to the risk assessment and differencing pre- and post-treatment estimates of risk. This approach can be used to compare the effectiveness of alternative treatment types (e.g., thinning versus prescribed fire) and to understand how treatment effectiveness differs across the landscape due to variation in biophysical conditions. Major fuel treatment constraints are quantified with spatial models of fuel treatment feasibility and cost. The WIT combines spatially explicit measures of fuel treatment risk mitigation, feasibility, and cost to optimize the location and type of treatment to minimize risk. At the large watershed scale, this is accomplished with a technology called linear optimization to sort through the many location and treatment type combinations. Intermediate products of the analysis – such as the estimated cost-effectiveness of risk reduction – convey similar information at a higher spatial resolution for project level planning and evaluation.

Assessing wildfire risk to water supplies and optimizing fuel treatment location and type are data and model intensive processes. The remainder of the user guide is dedicated to explaining the technical implementation of these processes in the WIT. Those interested in only a science summary of the process are referred to Gannon et al. (2019).

## WIT Modeling Workflow

The WIT is constructed in three modules to address the ordered tasks of assessing wildfire risk to water supplies, planning an efficient mitigation program, and evaluating the performance of completed or candidate projects.

### Water Supply Risk Assessment

The WIT uses a linked model approach to quantify wildfire-water supply risk in terms of expected sediment impact costs to water supplies (Figure 2). This module also estimates post-treatment risk for any candidate fuel treatments. Several of the intermediate products are also made available for additional data viewing and analysis.

*Process summary*

Burn probability, modeled with the large fire simulator (FSim; Finney et al. 2011) by Short et al. (2020), is used to characterize fire likelihood and how it varies across the watersheds. Crown fire activity modeled with FlamMap 5.0 (Finney et al. 2015) is used as a proxy for burn severity by mapping surface, passive crown, and active crown fire to low, moderate, and high severity, respectively. Post-fire hillslope erosion is then modeled with a Geographic Information System (GIS) implementation (Theobald et al. 2010) of the Revised Universal Soil Loss Equation (RUSLE; Renard et al. 1997) by altering cover and soil erodibility factors to reflect post-fire conditions (Larsen and MacDonald 2007). An empirical model of post-fire hillslope sediment delivery ratio (Wagenbrenner and Robichaud 2014) is used to predict how much of the eroded sediment is delivered to the stream and a conceptual model of channel sediment delivery ratio (Frickel et al. 1975), adapted to the channel types in the watersheds, is used to predict the total sediment delivery to the affected downstream water supplies. Water supply sediment exposure is quantified in metric tons (or megagrams [Mg]) and translated to a monetary value of impact with stakeholder defined sediment impact costs in USD per Mg of sediment. Data and modeling details are presented in Appendix I.

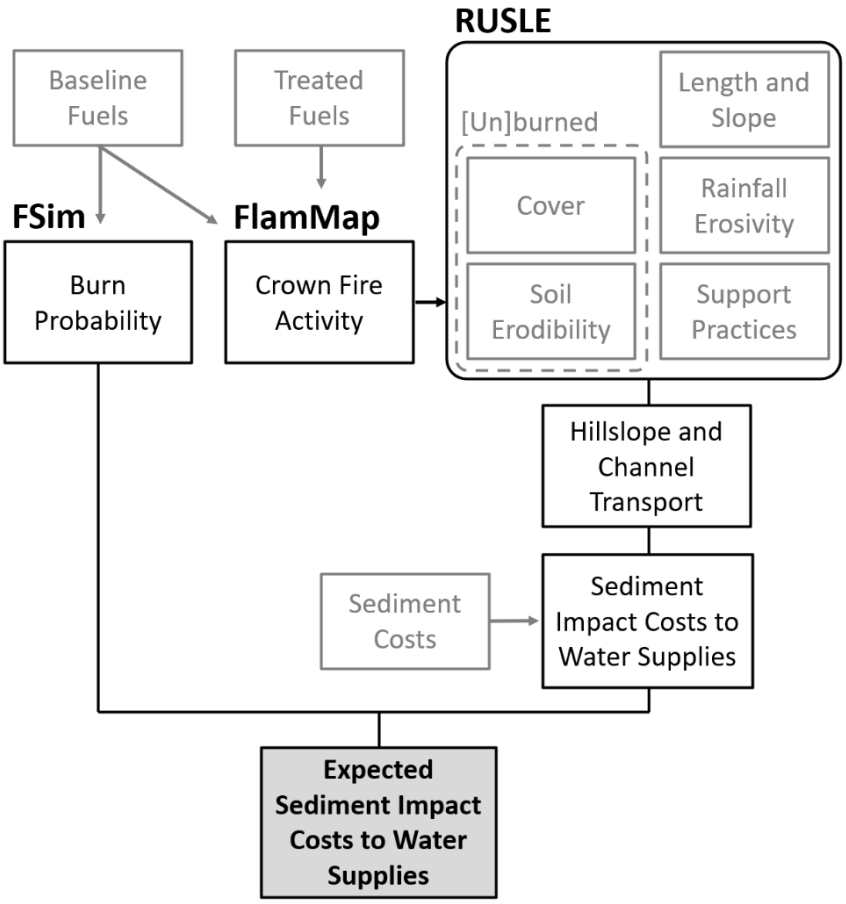


*Figure 2: The wildfire-water supply risk assessment uses modeled crown fire activity as a proxy for burn severity to modify cover and soil variables in the Revised Universal Soil Loss Equation (RUSLE) to estimate post-fire hillslope erosion, which is then routed off hillslopes and down channels to estimate sediment delivery to water supplies. Sediment yield is then combined with stakeholder-defined sediment impact costs to measure the conditional impact costs of fire, which are combined with burn probability to calculate the expected sediment impact costs.*

The wildfire-water supply risk assessment is implemented in the WIT with a combination of pre-processed and dynamic inputs designed to simplify the user experience and reduce computing needs. Several pre-processing steps are performed to generate a customized watershed network for the sediment transport modeling. All the baseline (pre-fire) inputs to RUSLE are pre-processed using ArcGIS 10.3 (ESRI 2015). See Appendix I for more details. The dynamic inputs to the model provide the ability to add or remove water supplies from the risk assessment and to modify their sediment impact costs.

*User input*


The moderate resolution National Hydrography Dataset Plus watershed network (NHDPlus; USEPA and USGS 2012) is used to represent the spatial topology between upland sediment sources and downstream water supplies via their connecting overland and channel flow paths. Overland flow paths are represented with pre-processed terrain analysis of a digital elevation model as described in Appendix I. The sediment contributed from each of many catchments (sub-watersheds) is routed through the flowline (channel) network to any downstream water supplies as indicated in Figure 3.

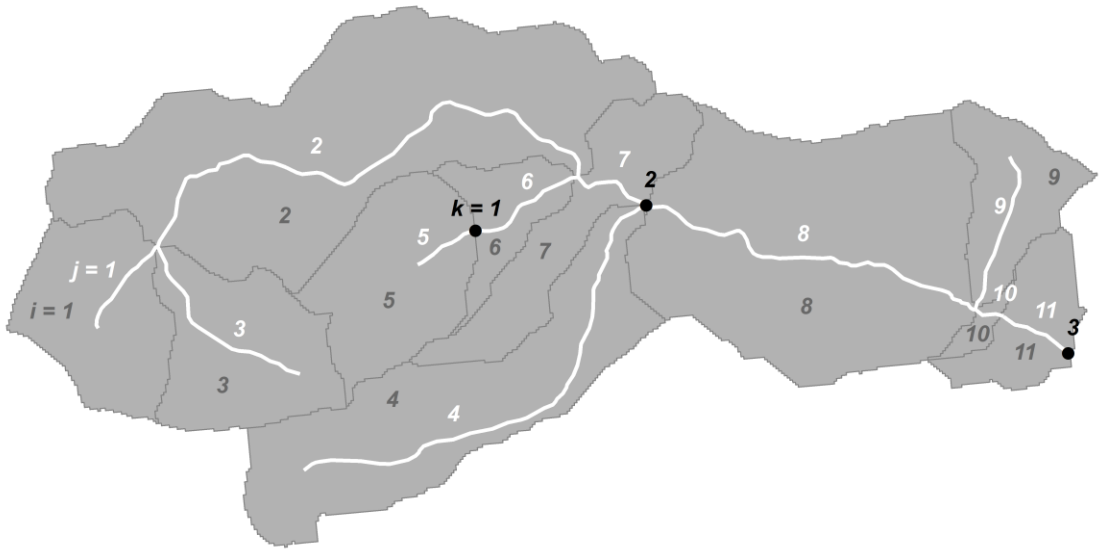


*Figure 3: Simplified example of the NHDPlus network topology. The matching catchment (i) and flowline (j) indices are used to associate upland sediment sources with their corresponding connections to the stream network. Water supplies, which we index in this example with k, are referenced to the appropriate flowline endpoint in the network.*

The user can add or remove water supplies from the risk assessment by modifying the infrastructure connections table (Table 1). This table specifies the name of the infrastructure component and the associated flowline(s) that best represent its connectivity to the NHDPlus watershed network. The flowline identifier (COMID) can be identified by viewing the flowline feature class from the input geodatabase in a GIS.

*Table 1: Example of the infrastructure connections table specifying the NHDPlus flowline that each feature of concern is connected to. When appropriate, features can be represented by multiple flowlines (e.g. Carter Lake).*

| Feature of Concern (FoC) | COMID |
|---|---|
| BARNES DITCH | 12808 |
| BARNES MEADOW RES | 2900901 |
| BIG BEAVER RES | 999000002 |
| CARTER LAKE RES | 13672 |
| CARTER LAKE RES | 13774 |
| CHAMBERS LAKE RES | 2900897 |
| COMANCHE RES | 2900919 |
| DILLE TUNNEL | 13544 |
| DIXON CANON RES | 999000004 |
| EAST PORTAL RESERVOIR | 999000008 |

The user can also modify the sediment impact costs (USD per Mg of sediment) assigned to the water supply infrastructure using the sediment costs table (Table 2). The pre-configured values were developed in a collaborative process with input from the city utilities of Fort Collins, Greeley, and Loveland and the Northern Water Conservancy District (Northern Water). Representatives from each agency rated the significance of sediment impacts to their infrastructure on a scale from 0 for no impact to 1 for highest level of impact. The impact costs were determined by summing the city utilities' impact ratings and multiplying them by baseline impact costs of 4, 8, and 15.6 USD $Mg^{-1}$ for primarily agricultural diversions, primarily drinking water diversions, and reservoirs, respectively. Setting a sediment impact cost to zero in this table is equivalent to removing it from the infrastructure connections table; this method is preferred when the goal is to narrow the focus of the assessment to a subset of water supplies.

*Table 2: Example of the sediment costs table specifying the sediment impact cost to each feature of concern in USD per Mg (metric ton). The feature of concern names must exactly match those used in the infrastructure connections table. An alias field is also provided as an option to abbreviate the names in the summary graphics.*

| Feature of Concern (FoC) | Alias | Cost per Ton (CostPerTon) |
|---|---|---|
| BARNES DITCH | BARNES DITCH | 8.0 |
| LOVELAND PIPELINE | LOVELAND PIPELINE | 1.6 |
| GEORGE RIST DITCH | GEORGE RIST DITCH | 0.0 |
| DILLE TUNNEL | DILLE TUNNEL | 5.0 |
| MARY S LAKE AT ESTES PARK | MARY'S LAKE AT ESTES PARK | 35.9 |
| EAST PORTAL RESERVOIR | EAST PORTAL RES | 37.5 |
| PINEWOOD RESERVOIR | PINEWOOD RES | 32.8 |
| LAKE ESTES | LAKE ESTES | 34.4 |
| CARTER LAKE RES | CARTER LAKE RES | 34.4 |
| POUDRE VALLEY CANAL | POUDRE VALLEY CANAL | 1.6 |

*Running the model*

The model first configures the watershed network based on the provided water supply infrastructure connections and values. It then combines the modeled crown fire activity from FlamMap with the pre-processed RUSLE inputs to estimate post-fire increase in erosion for the baseline and any post-treatment fuel scenarios. The post-treatment fuel scenarios are described in further detail in the fuel treatment optimization section. Sediment delivery to water supply infrastructure is then predicted by combining hillslope and channel sediment delivery ratio models. Mass of sediment delivered to infrastructure is then linked to the sediment impact costs (Table 2) to quantify the conditional impacts of fire in monetary terms. In the final step, conditional impacts are weighted by burn probability to estimate risk. Several intermediate products including raster layers of post-fire erosion, sediment delivery to streams, connectivity to water supplies, conditional water supply impacts, and water supply risk are saved to the output folder for viewing and critique in a GIS. These same products are also mapped for a quick inspection of the results.

*Results*

The model outputs include raster GIS files and static maps for viewing and critiquing the results of the water supply risk assessment (Figure 4). Advance users can load the raster data into a GIS for custom mapping or analysis. A set of static maps are also produced to make viewing the results convenient for users with less GIS skills. A common theme for maps is that impacts are mapped to the source locations to support watershed management planning. Risk is accounted for by water supply in the results for the later fuel treatment optimization module.

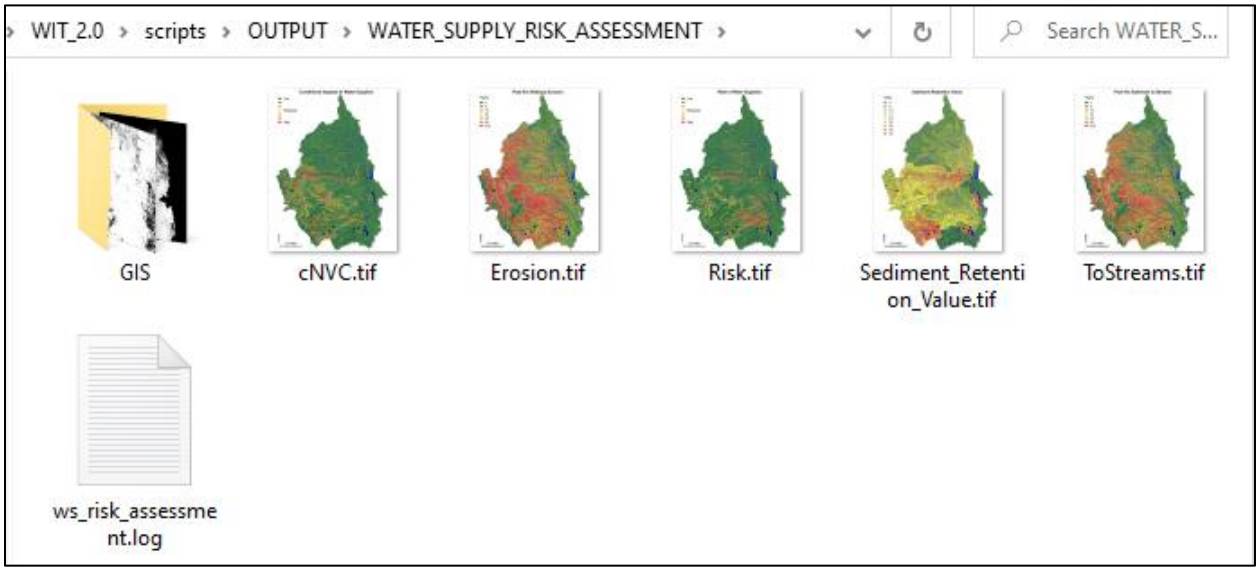


*Figure 4: Outputs of the water supply risk assessment include raster GIS files and static maps for viewing and critiquing the results.*

The first and most important output to critique is the sediment retention value map (Figure 5), which translates the two user inputs (Table 1; Table 2) into a spatial representation of watershed value. The values in this map should be interpreted as the avoided downstream cost if a metric ton (Mg) of sediment were retained in each catchment. Critique the map to make sure all water supplies are connected to the network and valued properly. The next two maps summarize the erosion and hillslope sediment transport model results for median rainfall conditions (Figure 6) to communicate how the components of the model combine to influence the final risk measures and for the interested user to compare the results to published studies. The final two maps present the conditional wildfire impacts and risk to water supplies (Figure 6), which relate the predicted mass of sediment delivered to water supplies to the assigned sediment impact costs. The risk map also incorporates the likelihood of each source pixel burning. The native units for both these data products are USD $ac^{-1}$, but they are presented in relative terms here for ease of communication with diverse audiences. All else equal, areas with high risk will be identified as priorities for fuels reduction treatments in the later fuel treatment optimization module.

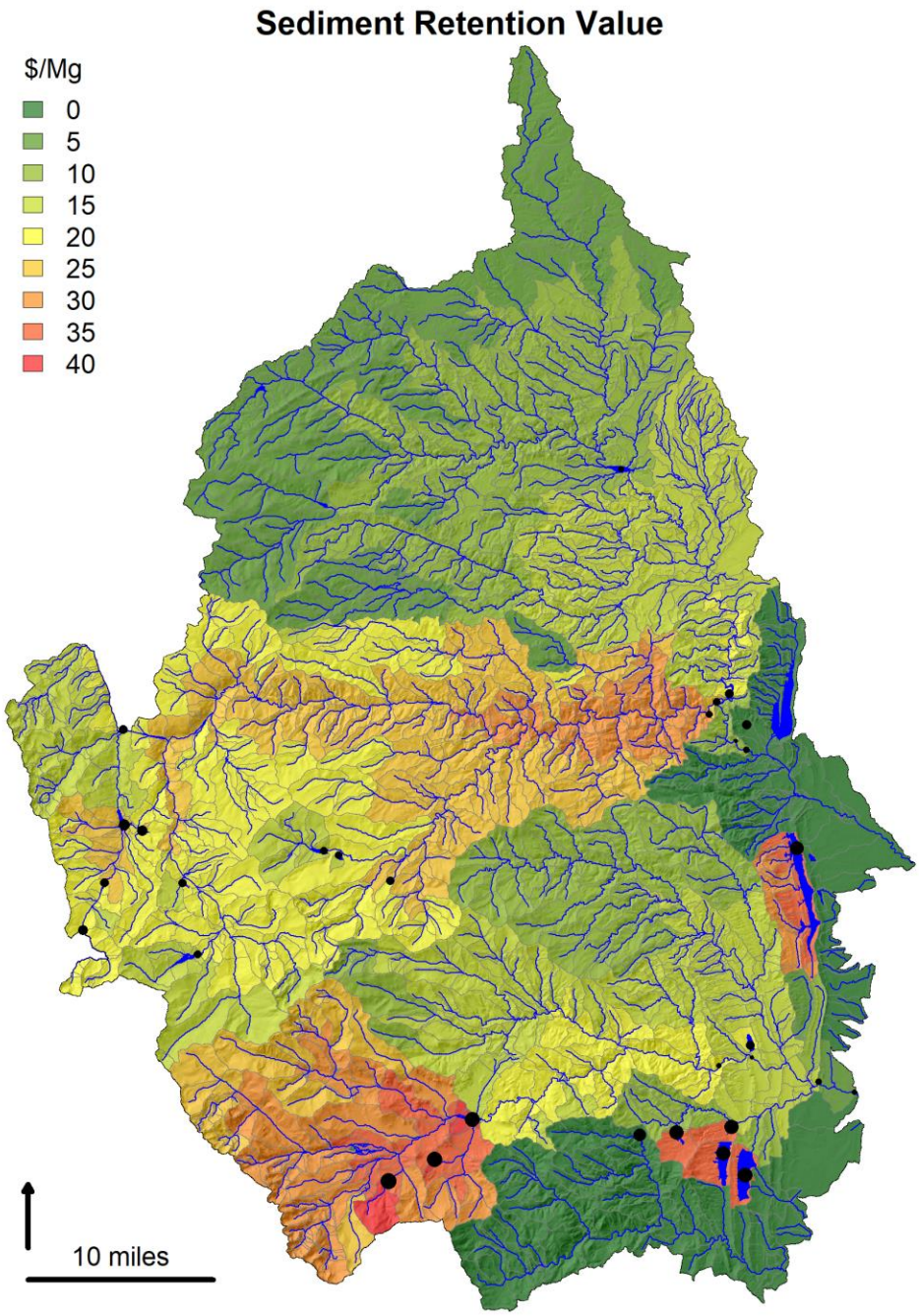


*Figure 5: The sediment retention value map combines the channel sediment delivery ratio model and the sediment impact costs to map the value of retaining a metric ton of sediment in each catchment. Water supplies are represented as black dots with the size corresponding to the assigned impact cost.*

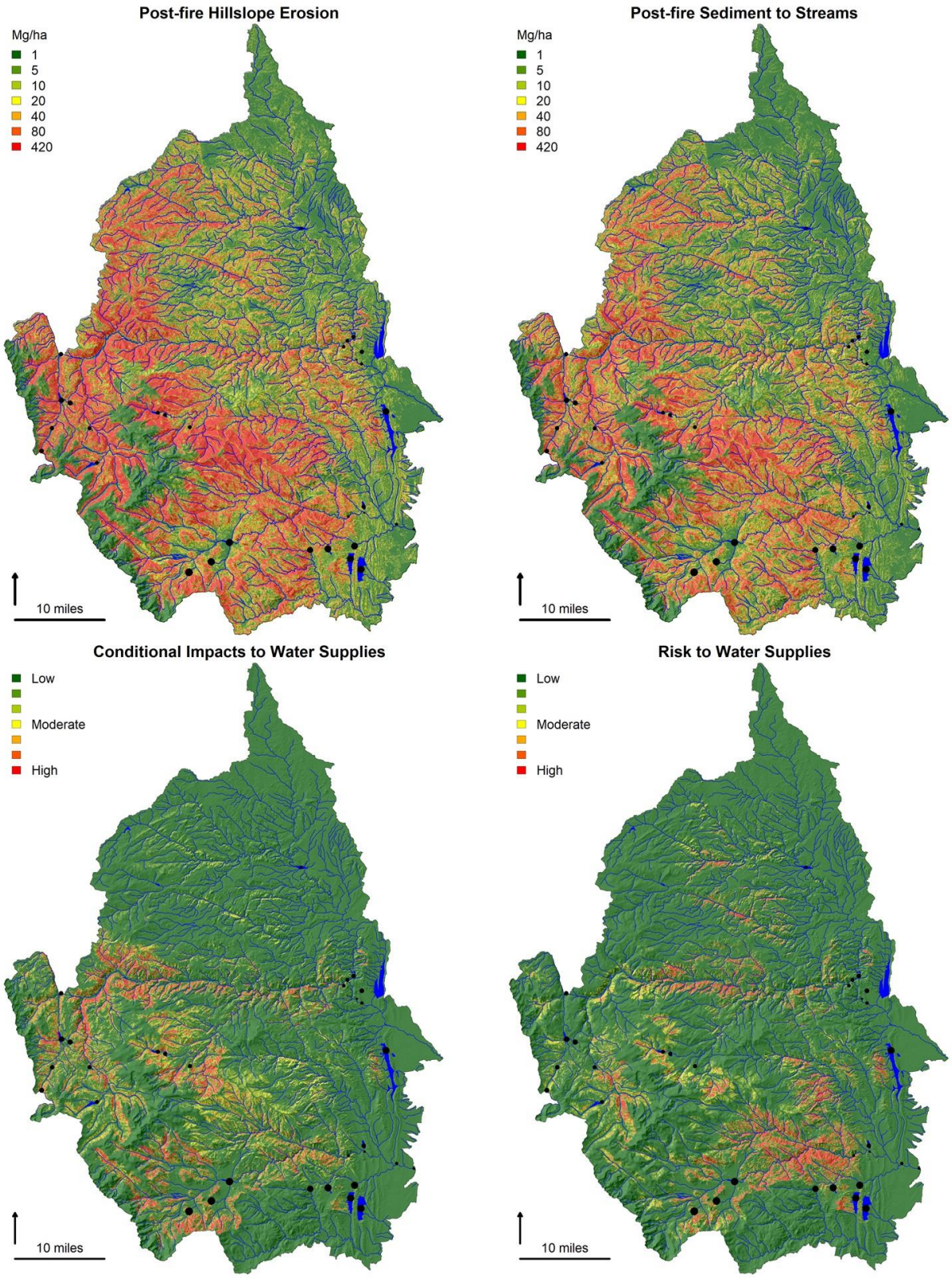


*Figure 6: Post-fire hillslope erosion (TOP LEFT) and sediment delivery to streams (TOP RIGHT) predictions account for three-years of increased gross sediment production. Units are Mg ha$^{-1}$ to facilitate comparisons with published studies. Conditional (BOTTOM LEFT) and expected (BOTTOM RIGHT) impacts to water supplies are calculated by relating the mass of sediment delivered to water supplies to their assigned impact costs.*

## Fuel Treatment Optimization

The WIT optimizes the location and type of fuel treatment using linear optimization, which is well-suited to evaluating a large set of candidate decision units based on their cost-effectiveness and adherence to planning constraints. The optimization module also produces several intermediate raster products that are made available for additional data viewing and analysis.

*Process summary*

The linear optimization model is designed to maximize water supply risk reduction (minimize risk) for a set of decision units representing the amount of treatment to allocate (ac) by location and type (Figure 7). The detailed mathematical formulation is provided in Appendix II. The decision units are evaluated in terms of their cost-effectiveness at reducing risk by assigning each treatment location and type the average treatment risk reduction (USD $ac^{-1}$) and cost (USD $ac^{-1}$) within the unit. NHDPlus (USEPA and USGS 2012) catchments are used as the treatment units, which vary in size from 0.5-8,800 ac with a mean of 650 ac in Northern Colorado. Due to variable conditions within the catchments, mean risk reduction and cost calculations are limited to the area modeled as feasible and effective for each treatment type. In this context, effective means lowers fire severity at least one category. Risk reduction is automatically calculated by treatment type from the water supply risk assessment outputs. Treatment feasibility and cost estimates are provided as raster surfaces by the analyst; the modeling for Northern Colorado is described in Appendix II. Three main constraints are considered in the model. The most important is that spending cannot exceed the total program budget (USD). Treatment is also limited at the catchment-level to the total area feasible by treatment type as well as the combined area feasible for all treatment types. This allows multiple treatment types to be assigned to the same unit so long as their extents do not overlap. The primary output of the optimization model is a treatment plan specifying the area assigned to each location and treatment type and the associated level of predicted risk reduction. Raster cost-effectiveness surfaces are also generated for each treatment type by dividing risk reduction by treatment cost.

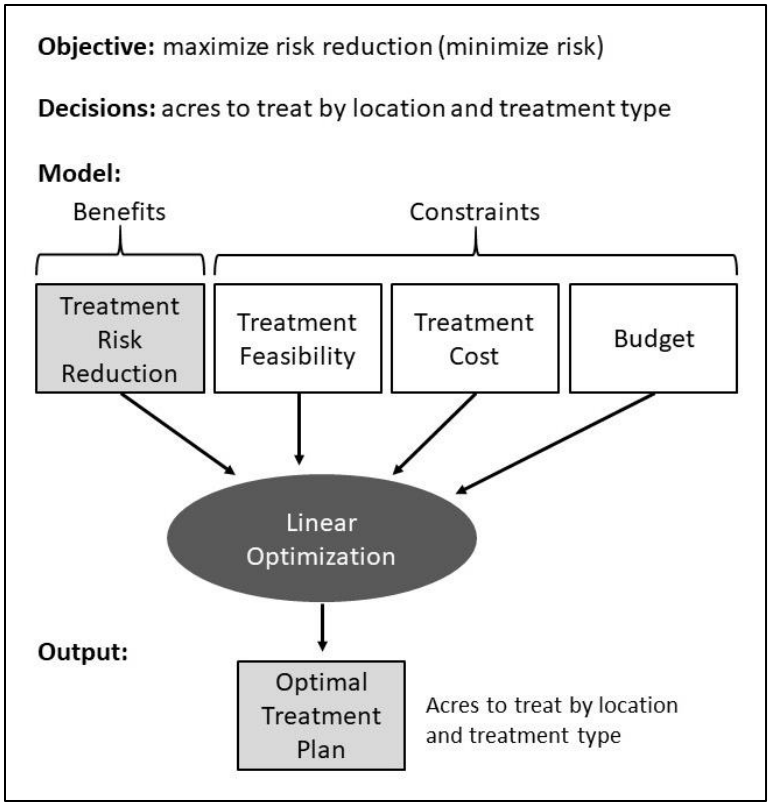


*Figure 7: Conceptual diagram summarizing how information is synthesized in linear optimization to prioritize treatment location and type to minimize risk.*

*User input*

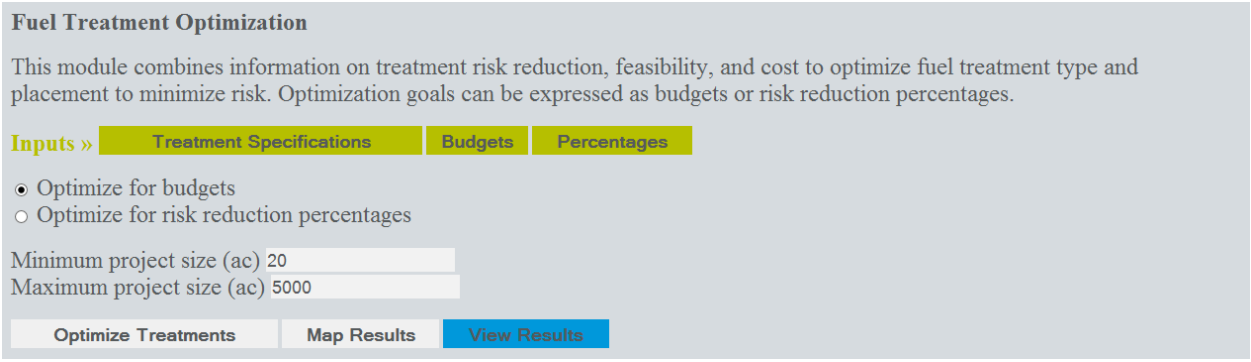


Three controls are provided to the user. The first is a treatment specifications table (Table 3). This is used to adjust the treatment types considered in the model and data sources used to represent their risk reductions, feasibilities, costs, and how outputs are labeled. GeoTIFF is the required format for raster inputs. The user can also modify a variable (MaxBudgetProp) to limit the proportion of the budget (0-1) that can be allocated to each treatment type to deal with unrealistic allocations. The model formulation requires the user to specify a program budget to constrain spending to. Two options are provided to specify the budget(s) to explore. The first is a budgets table (Table 4) that requires at least

one positive budget value (in USD) to run the model. Multiple values can be provided on separate rows to generate treatment plans at multiple budget levels with a single run. The second is a risk reduction percentages table (Table 5) that has equivalent function. The default is to use budgets, but the percentage option can be selected with the toggle switch. Size constraints can be imposed by entering values into the text boxes in the interface; treatment units with less feasible area than the minimum project size will not be considered for the treatment plan and catchment-level treatment allocations will not exceed the specified maximum project size.

*Table 3: Treatment specifications table. PT_Risk = post-treatment risk raster (USD $ac^{-1}$). T_Cost = treatment cost raster (USD $ac^{-1}$). T_Feas = treatment feasibility raster (0=infeasible;1=feasible). MaxBudgetProp = maximum budget proportion (value between 0 and 1). FB_Code = fire behavior code (unique name to associate fire modeling results and to tag model outputs with).*

| Treatment | PT_Risk | T_Cost | T_Feas | MaxBudgetProp | FB_Code |
|---|---|---|---|---|---|
| Thin | thin_eNVC.tif | mocost.tif | mofeas.tif | 1 | thin |
| Rx fire | RxFire_eNVC.tif | Rxcost.tif | Rxfeas.tif | 1 | RxFire |
| Complete | comp_eNVC.tif | mRxcost.tif | mofeas.tif | 1 | comp |

*Table 4: Budgets table. Budget = budget(s) to run the model at. A treatment plan will be constructed for each specified budget. Commas are shown here for ease of reading, but the actual file should include the values as raw numbers instead of formatted text. Priority = text name for the budget scenario for later mapping. Lower budgets correspond to higher treatment priority.*

| Budget | Priority |
|---|---|
| 10,000,000 | Highest |
| 50,000,000 | Higher |
| 100,000,000 | High |
| 200,000,000 | Moderate |

*Table 5: Risk reduction percentages table. PerRed = percentage(s) of risk reduction to run the model at. A treatment plan will be constructed for each specified percentage. Priority = text name for the percentage scenario for later mapping. Lower percentages correspond to higher treatment priority.*

| PerRed | Priority |
|---|---|
| 5 | Highest |
| 10 | Higher |
| 15 | High |
| 20 | Moderate |

The most important inputs to the optimization model are the raster surfaces of treatment risk reduction, cost, and feasibility. A brief description of how these are generated is provided here with details reserved for Appendix II. Risk reduction estimates are generated in the WIT by providing modeled crown fire activity for each candidate treatment as input to the previously described water supply risk assessment module. The risk assessment module identifies the candidate treatments to evaluate using the treatment specifications table (Table 3). Post-treatment risk is then subtracted from baseline risk in

the optimization module to estimate risk reduction in USD $ac^{-1}$ over a 25-year planning period. Treatment cost surfaces should have units of USD $ac^{-1}$. For Northern Colorado, thinning costs are estimated to increase with distance from roads and slope steepness with a function that predicts costs between 2,500 and 10,000 USD $ac^{-1}$. Prescribed fire costs are estimated at a flat rate of 1,000 USD $ac^{-1}$. The cost of a complete treatment combining thinning and prescribed fire is calculated as the sum of thinning and prescribed fire costs. Here, feasibility refers to a binary layer depicting where a given treatment is possible (1) or not possible (0) based on hard constraints. Accessibility and operability constraints are already factored into the cost estimates. All treatments are restricted to forested areas. Thinning treatments are further limited from areas protected with wilderness and upper tier roadless designations. Prescribed fire is constrained to frequent-fire forests greater than 250-m away from structures in the wildland-urban interface.

*Running the model*

The model first reads in the spatial inputs and then summarizes treatment risk reduction, cost, and feasibility for each treatment type and unit. As previously mentioned, estimates of average risk reduction and cost are limited to the area feasible for that treatment type. Prior to formulating the model, any decision units with less feasible area than the minimum project size are removed from consideration and any units with more than the maximum project size are constrained the maximum by adjusting the feasible area in the unit. Optimization is performed with the free lp_solve program (http://web.mit.edu/lpsolve_v5520/doc/index.htm), which requires the data be manipulated into vector and matrix form to describe the objective function values and constraints for each decision unit. An avoided impact analysis is performed across the full range of possible budgets to communicate how risk reduction and treatment type allocations will vary at untested budget levels. If the risk reduction percentage option is selected, the results of the avoided impact analysis are used to identify the budget needed to meet the risk reduction goal. The module then solves the linear program for each budget level and saves the associated treatment plan describing the area assigned to each treatment type and unit. Risk reduction and treatment allocation by budget level is also summarized in a table.

*Results*

The model outputs include tabular and vector GIS files (shapefiles) of the optimal treatment plan for each budget, a summary table of results by budget, and a figure summarizing the results of the avoided impact analysis (Figure 8).

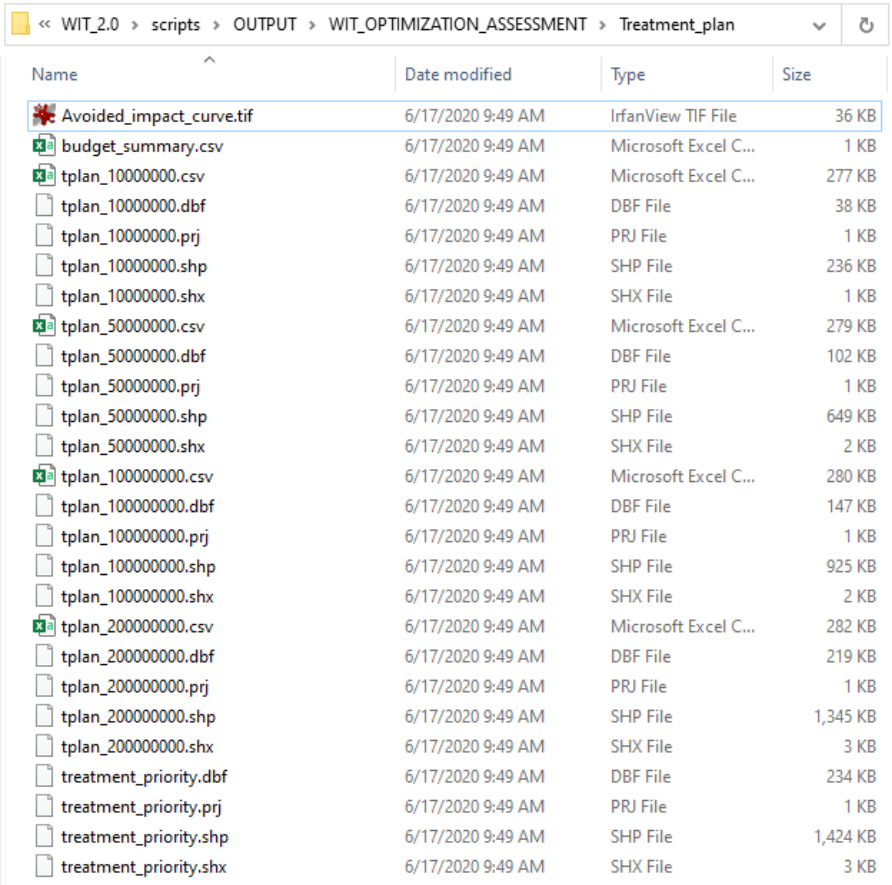


*Figure 8: Outputs of the fuel treatment optimization include tabular and vector GIS files (shapefiles) depicting the optimal treatment plan for each budget, a treatment priority shapefile, a summary table of results by budget, and the avoided impact analysis results. Budget levels (USD) appear in the treatment plan file names.*

The optimal treatment plan is communicated in a long-form table (Table 6) and a wide-form shapefile (Figure 9). In the long-form table, each spatial treatment unit (*UID* field) will have multiple rows corresponding to the number of treatment types considered in the assessment (Table 3). The selected locations and treatment types can be identified by filtering for decision units with allocated treatment (> 0 in *Acres* field). The treatment type codes correspond to the order that treatments are presented in Table 3. The optimal treatment plan is also communicated in a shapefile with a wide-form attribute table (Figure 9). Only treatment units selected by the model appear in the output. The treatment priority shapefile flattens the treatment plans for all budgets and assigns each catchment the highest priority level (from Table 4 or Table 5) that it is selected for treatment at.

*Table 6: Optimal treatment plan table. UID = unique identifier for treatment unit. FEATUREID & GRIDCODE = unique identifiers for NHDPlus catchments. TotFeasAcre = total feasible acres in catchment for any treatment type. FeasAcre = feasible acres in catchment for specified treatment type. RedPerAcre = average treatment risk reduction (USD ac$^{-1}$). CostPerAcre = average treatment cost (USD ac$^{-1}$). TrtType = numerical code corresponding to row numbers in Table 3. Acres = planned allocation of treatment.*

| UID | FEATUREID | GRIDCODE | TotFeasAcre | FeasAcre | RedPerAcre | CostPerAcre | TrtType | Acres |
|---|---|---|---|---|---|---|---|---|
| 0 | 12680 | 789308 | 17.1 | 0.0 | 2.4 | 2,500.0 | 1 | 0.0 |
| 0 | 12680 | 789308 | 17.1 | 0.0 | 8.4 | 1,000.0 | 2 | 0.0 |
| 0 | 12680 | 789308 | 17.1 | 0.0 | 1.2 | 3,500.0 | 3 | 0.0 |
| 1 | 13582 | 789322 | 571.1 | 299.6 | 85.0 | 2,748.7 | 1 | 0.0 |
| 1 | 13582 | 789322 | 571.1 | 66.9 | 71.1 | 1,000.0 | 2 | 66.9 |
| 1 | 13582 | 789322 | 571.1 | 570.0 | 58.6 | 3,711.4 | 3 | 0.0 |
| 2 | 12554 | 789329 | 3.8 | 0.0 | 3.3 | 2,500.0 | 1 | 0.0 |
| 2 | 12554 | 789329 | 3.8 | 0.0 | 0.0 | 999,999.0 | 2 | 0.0 |
| 2 | 12554 | 789329 | 3.8 | 0.0 | 5.3 | 3,506.7 | 3 | 0.0 |
| 3 | 11010 | 789340 | 371.6 | 174.4 | 23.1 | 2,773.3 | 1 | 0.0 |
| 3 | 11010 | 789340 | 371.6 | 75.2 | 13.8 | 1,000.0 | 2 | 0.0 |
| 3 | 11010 | 789340 | 371.6 | 370.3 | 14.2 | 3,702.9 | 3 | 0.0 |

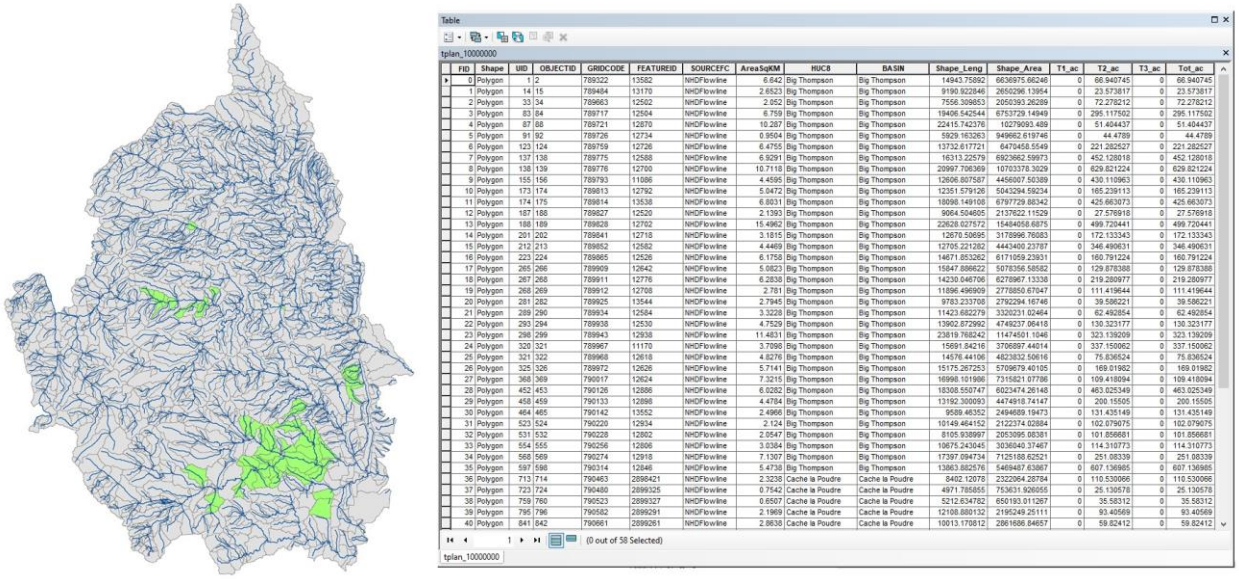


*Figure 9: Optimal treatment plan shapefile. The module will produce a treatment plan shapefile for every budget. T1_ac = area allocated to treatment type one from Table 3. Tot_ac = total treatment area allocated to unit.*

The budget summary table is designed to compare performance metrics and treatment allocations across budget levels (Table 7). It describes how much risk is mitigated at each budget level in USD (*ObjVal* field), percent of the baseline total (*PerRR* field), and percent of the maximum feasible risk reduction considering the feasibility and project size constraints in the model (*PerMFRR* field). It also reports how much of each treatment type is utilized in terms of both area (e.g., *T1_acres* field) and budget (e.g., *T1_USD* field).

*Table 7: Budget summary table. Budget = treatment budget (USD). ObjValue = risk reduction objective value (USD). T1_acres = area allocated to treatment type 1 from Table 3. T1_USD = budget (USD) allocated to treatment type 1 from Table 3. PerRR = percent of total risk reduced. PerMFRR = percent of maximum feasible risk reduction. For the risk reduction percentage option, PerRed = the input percentage goal.*

| Budget | ObjVal | T1_acres | T1_USD | T2_acres | T2_USD | … | PerRR | PerMFRR |
|---|---|---|---|---|---|---|---|---|
| 10,000,000 | 878,280 | 0 | 0 | 10,000 | 10,000,000 | | 7.4 | 13.3 |
| 50,000,000 | 2,469,318 | 9,162 | 27,966,968 | 21,576 | 21,576,378 | | 20.8 | 37.4 |
| 100,000,000 | 3,695,309 | 23,005 | 68,903,585 | 28,809 | 28,808,984 | | 31.1 | 55.9 |
| 200,000,000 | 5,058,042 | 44,931 | 131,825,047 | 36,284 | 36,283,663 | | 42.5 | 76.4 |

The last product is a figure summarizing the results of the avoided impact analysis (Figure 10). This analysis first estimates a high-end budget that would result from treating all feasible area with the most expensive treatment type and then solves the linear program at many small budget increments up to the high-end budget. The top panel provides perspective about how the selected budget levels compare in terms of their cost-effectiveness at reducing risk and how much of the maximum mitigable risk they achieve. The bottom panel illustrates how treatment type allocations shift with changing budget. In this example, prescribed fire dominates when budgets are small because it is the most cost-effective treatment, but as budget because non-limiting, the treatment allocation shifts towards the complete treatment because it is most effective.

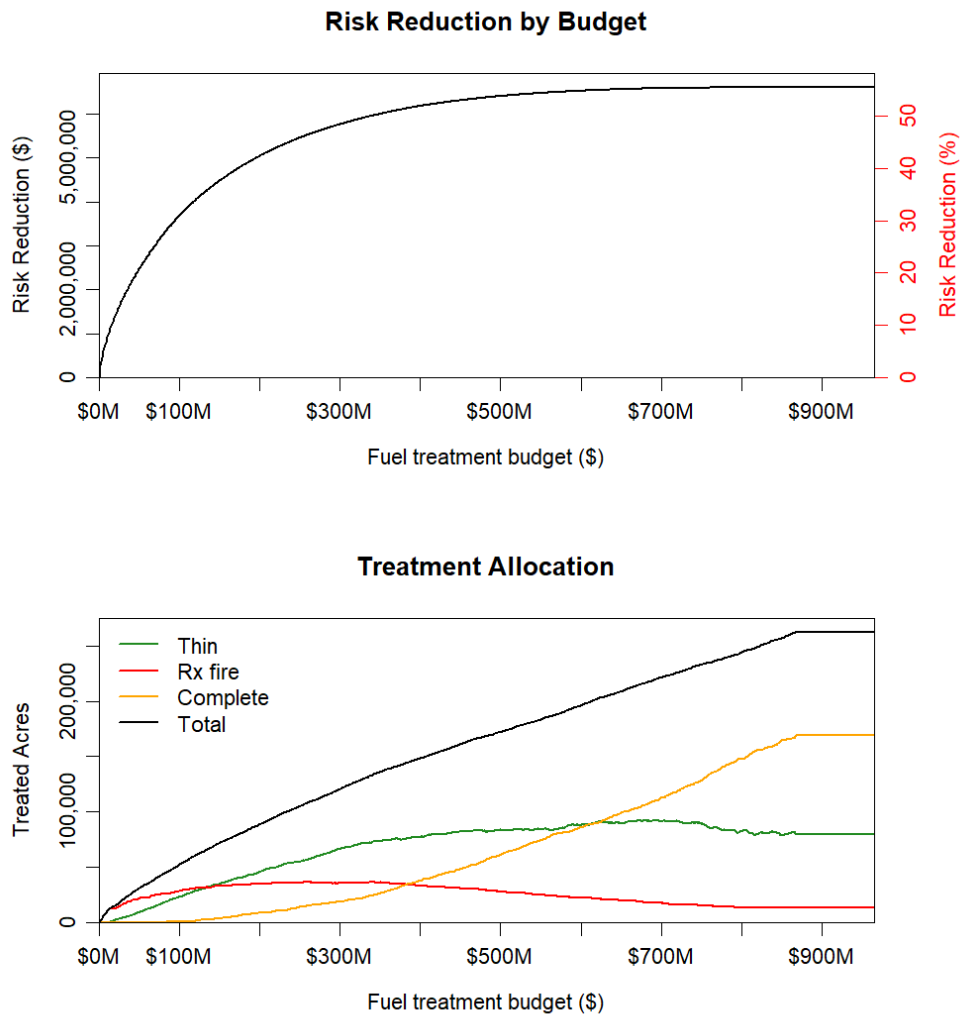


*Figure 10: Avoided impact analysis. The top panel displays how much risk reduction is achieved at various budget levels and the bottom panel displays the optimal treatment allocation by type. Risk reduction % in the top panel is of the total risk.*

### *Map results (optional)*

This optional post-optimization workflow performs basic mapping of the optimization inputs, intermediate products, and output treatment plans to make the spatial information accessible to users without strong GIS skills. This process is separated from the optimization model because of the significant time it takes to produce the graphics. Additionally, some intermediate products are provided as GIS files for custom mapping and analysis in GIS. The output directory separates the maps and supplementary GIS files (Figure 11).

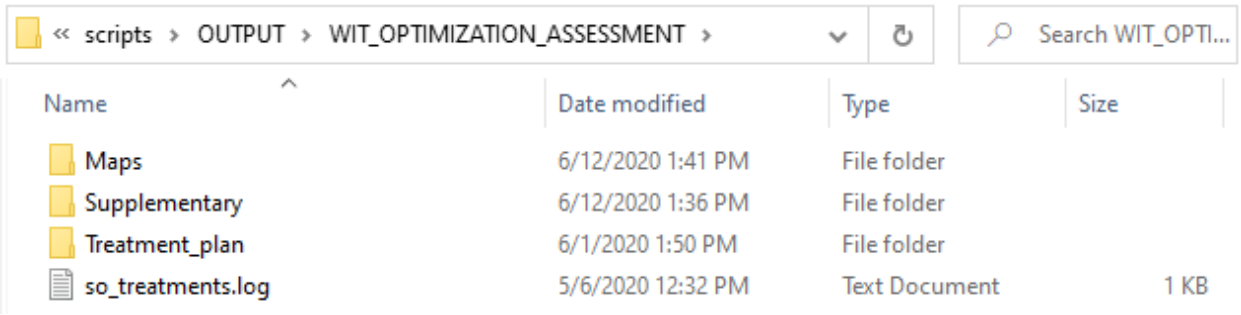


*Figure 11: Fuel treatment optimization output folder structure.*

The maps folder features several products (Figure 12). The treatment plan summary figures map each treatment plan and report on the water supply risk mitigation effects (TrtPlan_[BUDGET LEVEL].tif). If multiple budget levels are provided in Table 7, a priority map is generated using the assigned priority names (TrtPlans_priority.tif). Lower budget levels identify the highest priorities for treatment. For each candidate treatment type, maps are provided of the modeled risk reduction ([TREATMENT TYPE]_risk_reduction.tif), area feasible for treatment ([TREATMENT TYPE]_feasibility.tif), treatment cost ([TREATMENT TYPE]_cost.tif), and treatment cost-effectiveness ([TREATMENT TYPE]_cost_effectiveness.tif). Cost-effectiveness is calculated as treatment risk reduction divided by treatment cost.

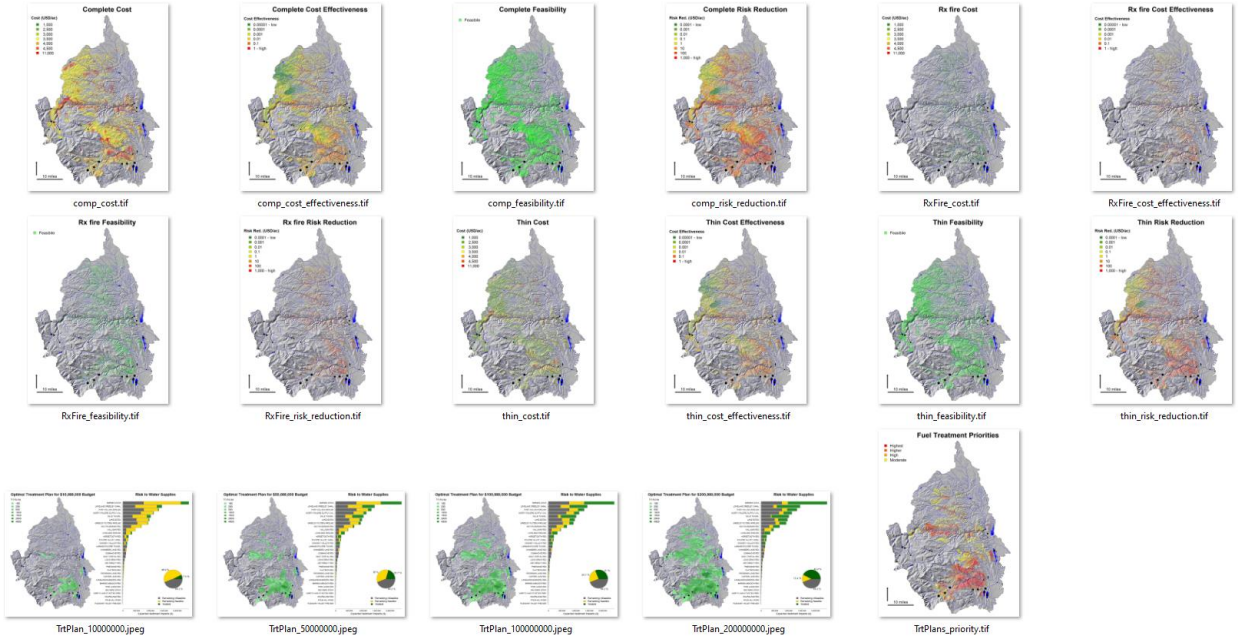


*Figure 12: Optional maps describing optimization model inputs, intermediate products, and treatment plan outputs.*

The supplementary GIS folder provides access to several of the intermediate and output products of the optimization (Figure 13). Rasters of treatment risk reduction and cost-effectiveness are provided for each treatment type ([TREATMENT TYPE]_RR.tif and [TREATMENT TYPE]_BCR.tif). The full attribute information used to parameterize the linear optimization program is provided in tabular (TrtUnit_metrics.csv) and shapefile format (TrtUnit_metrics.shp).

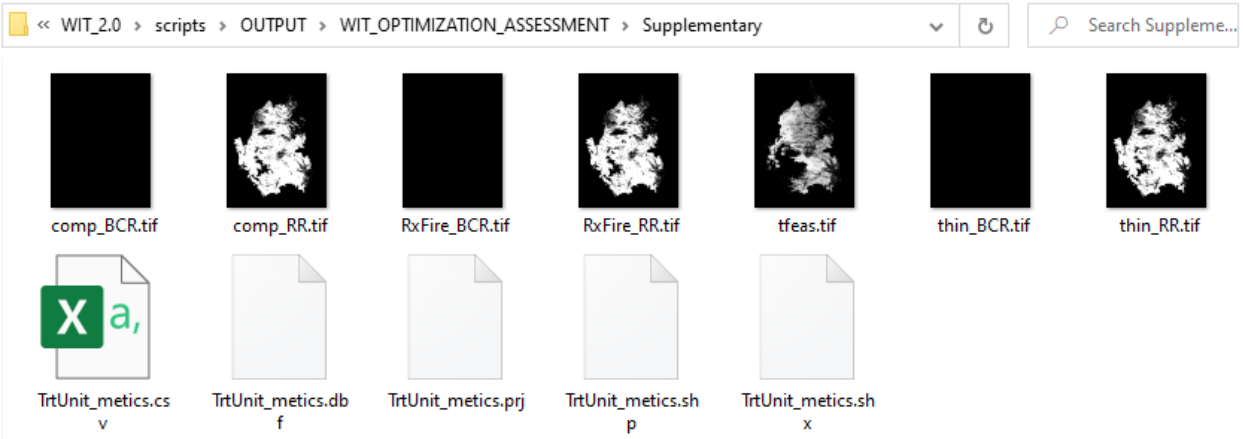


*Figure 13: Supplementary output folder containing spatial data for viewing or analysis in GIS.*

**Performance Metrics Assessment**

The WIT also calculates a suite of performance metrics for accomplished or planned fuels reduction work. This workflow is meant to complement the landscape-scale fuel treatment optimization by summarizing many of the intermediate products of the risk assessment and selected co-benefits related to home protection, recreation, and wildlife at a relevant scale for accomplishments reporting or evaluating proposed projects.

*Process summary*

This module ingests information describing the location and type of past or planned fuels reduction treatments and performs a series of spatial analyses to estimate performance measures for each treatment unit. This includes accounting of modeled effects on fire behavior, post-fire erosion, sediment load to streams, and water supply infrastructure exposure to sediment. This information is intended to help convey the project benefits to water stakeholders in multiple relevant terms. The assessment also accounts for several of the wildfire protection co-benefits of source water protection to homes, wildlife, and recreation. The full list of metrics, data sources, and analysis methods are described in Appendix III. Benefits are currently assessed using two different methods (Figure 14). The first is an analysis of avoided impacts based on the same foundational risk assessment principals used in the wildfire water supply risk assessment (Finney 2005; Scott et al. 2013) to estimate the conditional and expected impacts over a 25-year planning period. The second method is a simple overlay analysis to identify where treatments overlap resources of concern; depending on the data type, the resulting measures are either counts, lengths, or areas within the treated area or a defined buffer around the treated area.

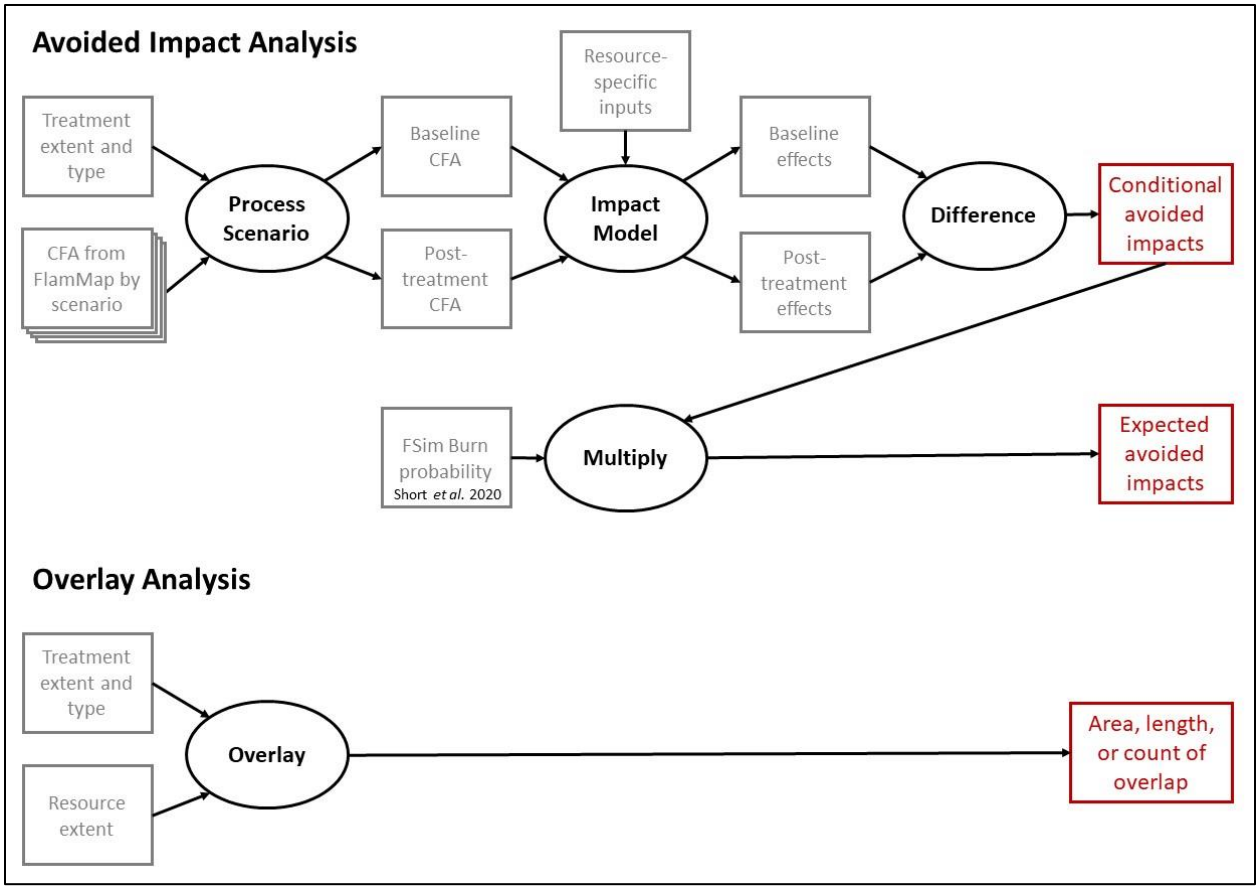


*Figure 14: Conceptual diagrams of the full avoided impact and overlay analyses used to quantify treatment co-benefits.*

*User input*

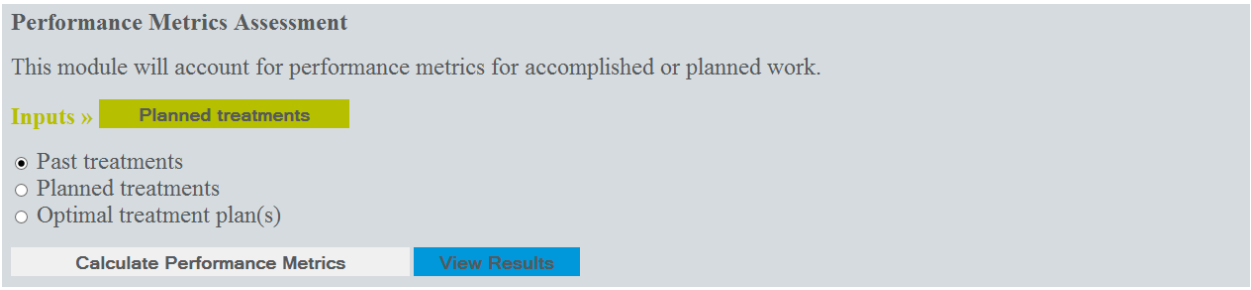


The only user input to the module is specifying which type of analysis to run. The *past treatments* option uses pre-processed data stored in the WIT to look at prior accomplishments by differencing current conditions from a 2016 baseline. Similarly, the *optimal treatment plan(s)* option directly accesses the output of the fuel treatment optimization module; the only requirement is that the optimization module has been successfully run first. The *planned treatments* option allows the user to make a forward-looking assessment of proposed treatments by differing hypothetical post-treatment conditions from the current baseline. This option requires a spatial treatment plan in ESRI

shapefile format to be provided in the folder pointed to in the user interface. The shapefile can be named whatever the user desires. Only one shapefile can be provided. The existing planned treatment shapefile should be used as a template for future revisions (Figure 15). The shapefile must include a text field describing the planned treatment type ("TrtType"). The allowable options are "Thin", "Rx fire", "Complete", and "Unknown" corresponding to the treatment types described in Appendix II. Spelling and capitalization must match. Treatments with "Unknown" type will be assessed as "Thin". No aggregation or disaggregation of polygons is performed by the tool. If multiple disjunct polygons should be assessed as a single unit, they should either be merged into a multi-part polygon before running the module, or metrics should be summarized for the multiple related entries in the output. Similarly, multi-part polygons need to be converted into single-part polygons by the user prior to using the tool if metrics are desired for each polygon. Although not required, it is strongly suggested that the treatment plan also include attributes necessary for sorting and summarizing the metrics such as a unique numerical identifier, project and treatment unit names, managing agency, funder, date, and a brief description of the proposed activities.

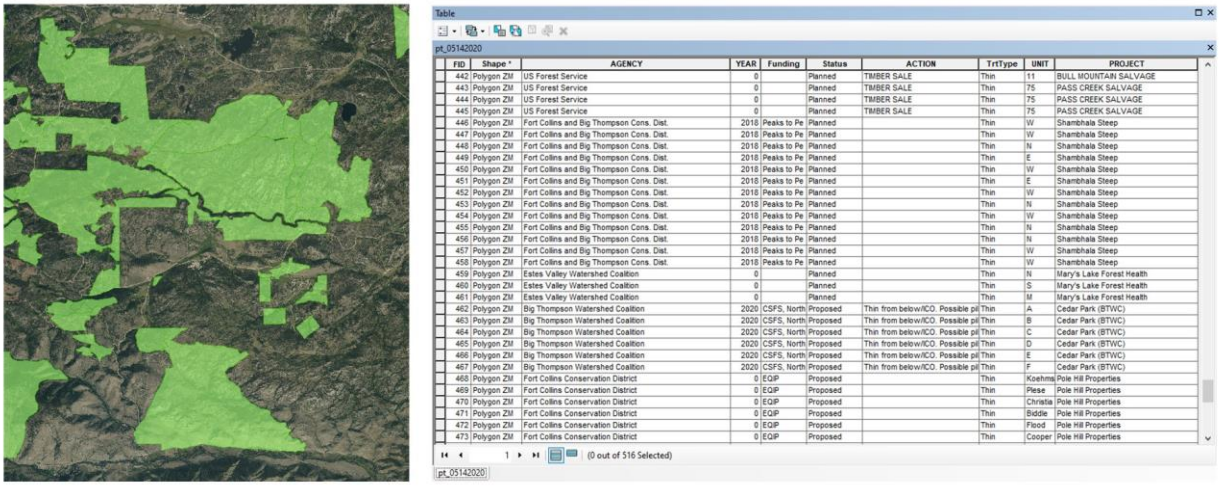


*Figure 15: Example planned treatment shapefile with the required "TrtType" field and optional summary attributes.2*

*Running the model*

The model first reads in the appropriate spatial representation of the treatment plan based on the user selected assessment type. Then, the appropriate baseline and post-treatment fire and erosion modeling products are assembled to represent the endpoints for the assessment. Consistent with the optimization module, the performance metrics for the optimal treatment plan input type will be assessed using the average effects for the selected treatment locations and types; this means the assessment models are run multiple times for every treatment unit, so expect long run times. Zonal statistics are used to aggregate metrics related to change in fire behavior, erosion, sediment delivery to infrastructure, and associated costs to the treatment units. Avoided impact and overlay analyses (Figure 14) are then performed for the co-benefits described in Appendix III. The

home loss model involves computationally intensive neighborhood analyses, so the assessment module is not quick; the analysis time should be in the range of 10-15 minutes on a high-performance computer. For the past and planned treatments, the output will include a single shapefile and spreadsheet table reporting the performance metrics. For the optimal treatment plan method, the output will instead include a shapefile and spreadsheet table for each budget level.

*Results*

The model outputs include both a table format for viewing in a spreadsheet program and shapefile viewing in a GIS (Figure 16). The performance measures are appended to the original attribute columns so the output can be filtered or summarized based on project, agency, or treatment type. Refer to the attribute key or descriptions provided in Appendix III on how to interpret the metrics. The output for the optimal treatment plan option will include additional outputs tagged with treatment type; these represent the average effects of applying each treatment type in each catchment. The optimal treatment plan option will also tag the performance metric tables with the budget level.

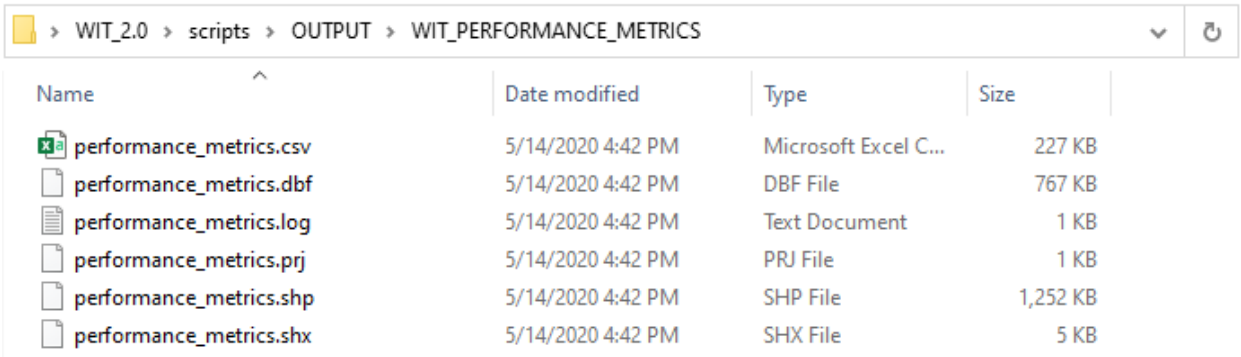


*Figure 16: Outputs of the performance metrics module include tabular and vector GIS files (shapefiles) depicting the treatment plan and associated performance metrics. The optimal treatment plan option will produce additional files depicting the average benefit for each treatment type in each unit and a composite of the selected treatment plan for each budget.*

Attributes beyond treatment type will prove useful for working with the model outputs. For example, metrics can be aggregated from treatment unit to project by summing most fields. For planned work, it may also be useful to sort and rank the candidate projects or treatment units by their benefit or cost effectiveness.

## References


Addington RN, Aplet GH, Battaglia MA, Briggs JS, Brown PM, Cheng AS, Dickinson Y, Feinstein JA, Pelz KA, Regan CM, Thinnes J, Truex R, Fornwalt PJ, Gannon B, Julian CW, Underhill J, Wolk B (2018) Principles and practices for the restoration of ponderosa pine and dry mixed-conifer forests of the Colorado Front Range. USDA Forest Service Rocky Mountain Research Station RMRS-GTR-373. 121 p. (Fort Collins, CO)

Agee JK, Bahro B, Finney MA, Omi PN, Sapsis DB, Skinner CN, van Wagtendonk JW, Weatherspoon CP (2000) The use of shaded fuelbreaks in landscape fire management. *Forest Ecology and Management* **127**, 55-66. doi:10.1016/S0378-1127(99)00116-4

Benavides-Solorio JD, MacDonald LH (2005) Measurement and prediction of post-fire erosion at the hillslope scale, Colorado Front Range. *International Journal of Wildland Fire* **14**, 457–474. doi:10.1071/WF05042

Bradshaw L, McCormick E (2000) FireFamily Plus user's guide, version 2.0. USDA Forest Service, Rocky Mountain Research Station, General Technical Report RMRS-GTR-67WWW. (Ogden, UT, USA)

Breiby T (2006) Assessment of soil erosion risk within a subwatershed using GIS and RUSLE with a comparative analysis of the use of STATSGO and SSURGO soil databases. Papers in Resource Analysis, Volume 8. Saint Mary's University of Minnesota Central Services Press. pp. 1–22. (Saint Mary's University of Minnesota Central Services Press: Winona, MN, USA)

Buckley M, Beck N, Bowden P, Miller ME, Hill B, Luce C, Elliot WJ, Enstice N, Podolak K, Winford E, Smith SL, Bokach M, Reichert M, Edelson D, Gaither J (2014) Mokelumne watershed avoided cost analysis: why Sierra fuel treatments make economic sense. A report prepared for the Sierra Nevada Conservancy, The Nature Conservancy, and USDA Forest Service. Sierra Nevada Conservancy. (Auburn, CA, USA)

Caggiano MD, Tinkham WT, Hoffman C, Cheng AS, Hawbaker TJ (2016) High- resolution mapping of development in the wildland–-urban interface using object- based image extraction. *Heliyon* **2**, e00174. doi:10.1016/j.heliyon.2016.e00174

Calkin D, Gebert K (2006) Modeling fuel treatment costs on Forest Service Lands in the Western United States. *Western Journal of Applied Forestry* **21(4)**, 217-221.

Calkin DE, Cohen JD, Finney MA, Thompson MP (2014). How risk management can prevent future wildfire disasters in the wildland-urban interface. *Proceedings of the National Academy of Sciences* **111(2)**, 746-751. doi:10.1073/pnas.1315088111

Cohen JD (2000). Preventing disaster: home ignitability in the wildland-urban interface. *Journal of Forestry* **98(3)**, 15-21. doi:10.1093/jof/98.3.15

Crosby JS, Chandler CC (1966) Get the most from your windspeed observation. *Fire Control Notes* **27**, 12–13.

Dabney S (2016) Rainfall intensity summarization tool (RIST), version 3.96. USDA Agricultural Research Service, National Sedimentation Laboratory. (Oxford, MS, USA)

DeBano LF, Neary DG, Ffolliott PF (2005) Soil physical processes. In 'Wildland fire in ecosystems: effects of fire on soils and water'. (Eds DG Neary, KC Ryan, LF DeBano) USDA Forest Service, Rocky Mountain Research Station, General Technical Report RMRS-GTR-42-Vol. 4. (Eds DG Neary, KC Ryan, LF DeBano) pp. 29–51. (Ogden, UT, USA)

Elliot WJ, Miller ME, Enstice N (2016) Targeting forest management through fire and erosion modelling. *International Journal of Wildland Fire* **25**, 876–887. doi:10.1071/WF15007

ESRI (2015) ArcGIS software, version 10.3. Available at https://www.esri.com/en-us/home. (Redlands, CA)

Fernandez C, Wu JQ, McCool DK, Stöckle CO (2003) Estimating water erosion and sediment yield with GIS, RUSLE, and SEDD. *Journal of Soil and Water Conservation* **58**, 128–136.

Ferro V, Porto P (200) Sediment Delivery Distributed (SEDD) Model. *Journal of Hydrologic Engineering* **5**, 411–422.

Fight RD, Hartsough BR, Noordijk P (2006) Users guide for FRCS: fuel reduction cost simulator software. USDA Forest Service, Pacific Northwest Research Station General Technical Report PNW-GTR-668. 23 p (Portland, OR)

Finney MA (2002) Fire growth using minimum travel time methods. *Canadian Journal of Forest Research* **32**, 1420-1424. doi:10.1139/X02-068

Finney MA (2005) The challenge of quantitative risk analysis for wildland fire. *Forest Ecology and Management* **211**, 97-108. doi:10.1016/j.foreco.2005.02.010

Finney M, Grenfell IC, McHugh CW (2009) Modeling containment of large wildfires using generalized linear mixed-model analysis. *Forest Science* **55**, 249–255.

Finney MA, McHugh CW, Grenfell IC, Riley KL, Short KC (2011) A simulation of probabilistic wildfire risk components for the continental United States. *Stochastic Environmental Research and Risk Assessment* **25**, 973–1000. doi:10.1007/s00477-011-0462-z

Finney MA, Brittain S, Seli RC, McHugh CW, Gangi L (2015) FlamMap: fire mapping and analysis system (version 5.0) [Software]. Available from http://www.firelab.org/document/flammap-software

Francis D, Ex S, Hoffman C (2018) Stand composition and aspect are related to conifer regeneration densities following hazardous fuels treatments in Colorado, USA. *Forest Ecology and Management* **409**, 417–424. doi:10.1016/J.FORECO.2017.11.053

Frickel DG, Shown LM, Patton PC (1975) An evaluation of hillslope and channel erosion related to oil-shale development in the Piceance basin, north-western Colorado. Colorado Department of Natural Resources, Colorado Water Resources Circular 30. (Denver, CO, USA)

Fu G, Chen S, McCool DK (2006) Modeling the impacts of no-till practice on soil erosion and sediment yield with RUSLE, SEDD, and ArcView GIS. *Soil & Tillage Research* **85**, 38-49. doi:10.1016/j.still.2004.11.009

Fulé PZ, Crouse JE, Roccaforte JP, Kalies EL (2012) Do thinning and/or burning treatments in the western USA ponderosa or Jeffrey pine-dominated forests help restore natural fire behavior? *Forest Ecology and Management* **269**, 68–81. doi:10.1016/j.foreco.2011.12.025

Gannon BM, Wei Y, MacDonald LH, Kampf SK, Jones KW, Cannon JB, Wolk BH, Cheng AS, Addington RN, Thompson MP (2019) Prioritising fuels reduction for water supply protection. *International Journal of Wildland Fire* **28**, 785-803. doi:10.1071/WF18182

Gannon BM (2020) Risk Assessment and Decision Support (RADS) Technical User Guide. Colorado Forest Restoration Institute at Colorado State University. (Fort Collins, CO, USA)

Graham RT (2003) Hayman Fire case study. USDA Forest Service, Rocky Mountain Research Station, General Technical Report RMRS-GTR-114. (Ogden, UT, USA)

Haas JR, Thompson M, Tillery A, Scott JH (2017) Capturing spatiotemporal variation in wildfires for improving post-wildfire debris-flow hazard assessments. In 'Natural hazard uncertainty assessment: modeling and decision support, geophysical monograph 223'. (Eds K Riley, P Webley, M Thompson) pp. 301–317. (John Wiley & Sons: Hoboken, NJ, USA)

Heinsch FA, Sikkink PG, Smith HY, Retzlaff ML (2018) Characterizing fire behavior from laboratory burns of multi-aged, mixed-conifer masticated fuels in the western United States. USDA Forest Service, Rocky Mountain Research Station, Research Paper RMRS-RP-107. (Fort Collins, CO, USA)

Henkle JE, Wohl E, Beckman N (2011) Locations of channel heads in the semiarid Colorado Front Range, USA. *Geomorphology* **129**, 309–319. doi:10.1016/j.geomorph.2011.02.026

Jones KW, Cannon JB, Saavedra FA, Kampf SK, Addington RN, Cheng AS, MacDonald LH, Wilson C, Wolk B (2017) Return on investment from fuel treatments to reduce severe wildfire and erosion in a watershed investment program in Colorado. *Journal of Environmental Management* **198**, 66–77. doi:10.1016/j.jenvman.2017.05.023

LANDFIRE (2016) Fuel, topography, existing vegetation type, and fuel disturbance layers, LANDFIRE 1.4.0., U.S. Geological Survey. Available online at: http://landfire.cr.usgs.gov/viewer/

LANDFIRE (2019) Fuel, topography and existing vegetation type layers, LANDFIRE 2.0.0., U.S. Geological Survey. Available online at: http://landfire.cr.usgs.gov/viewer/

Larsen IJ, MacDonald LH (2007) Predicting post-fire sediment yields at the hillslope scale: testing RUSLE and disturbed WEPP. *Water Resources Research* **43**, W11412. doi:10.1029/2006WR005560

Larsen IJ, MacDonald LH, Brown E, Rough D, Welsh MJ, Pietraszek JH, Libohova Z, Benavides-Solorio JD, Schaffrath K (2009) Causes of post-fire runoff and erosion: water repellency, cover, or soil sealing? *Soil Science Society of America Journal* **73**, 1393–1407. doi:10.2136/sssaj2007.0432

Litschert SE, Theobald DM, Brown TC (2014) Effects of climate change and wildfire on soil loss in the Southern Rockies ecoregion. *Catena* **118**, 206–219. doi:10.1016/j.catena.2014.01.007

McCool DK, Foster GR, Mutchler CK, Meyer LD (1989) Revised slope length factor for the Universal Soil Loss Equation. *Transactions of the American Society of Agricultural Engineers* **32**, 1571–1576. doi:10.13031/2013.31192

McCuen RH (1998) 'Hydrologic analysis and design, – second 2nd edition.' (Prentice-Hall: New Jersey, NJ, USA)

Miller JD, Nyhan JW, Yool SR (2003) Modeling potential erosion due to the Cerro Grande Fire with a GIS-based implementation of the Revised Universal Soil Loss Equation. *International Journal of Wildland Fire* **12**, 85–100. doi:10.1071/WF02017

Miller S, Rhodes C, Robichaud P, Ryan S, Kovecses J, Chambers C, Rathburn S, Heath J, Kampf S, Wilson C, Brogan D, Piehl B, Miller ME, Giordanengo J, Berryman E, Rocca M (2017) Learn from the burn: the High Park Fire 5 years later. USDA Forest Service, Rocky Mountain Research Station, Science You Can Use Bulletin, Issue 25. (Fort Collins, CO, USA)

Moody JA, Martin DA (2001) Initial hydrologic and geomorphic response following a wildfire in the Colorado Front Range. *Earth Surface Processes and Landforms* **26**, 1049–1070. doi:10.1002/esp.253

Moody JA, Martin DA (2009) Synthesis of sediment yields after wildland fire in different rainfall regimes in the western United States. *International Journal of Wildland Fire* **18**, 96–115. doi:10.1071/WF07162

Moriarty K, Cheng AS, Hoffman CM, Cottrell SP, Alexander ME (2019) Firefighter observations of "surprising" fire behavior in mountain pine beetle-attacked lodgepole pine forests. *Fire* **2**, 34. doi:10.3390/fire2020034

Morici K, Wolk B, Cannon JB, Gannon B, Addington R (2019) 2018 Ecological Monitoring Report for Peaks to People Water Fund Demonstration Sites. CFRI Monitoring Report. Colorado Forest Restoration Institute, Colorado State University, and the Peaks to People Science Team. 33 p. Available at https://cfri.colostate.edu/publications/

Nearing MA (1997) A single, continuous function for slope steepness influence on soil loss. *Soil Science Society of America Journal* **61**, 917–919. doi:10.2136/sssaj1997.03615995006100030029x

NRCS Soil Survey Staff (2016) Web soil survey. USDA Natural Resources Conservation Service. Available online at: https://websoilsurvey.nrcs.usda.gov/

Parisien M-A, Dawe DA, Miller C, Stockdale CA, Armitage OB (2019) Applications of simulation-based burn probability modelling: a review. *International Journal of Wildland Fire* **28**, 913-926. doi:10.1071/WF19069

Perica S, Martin D, Pavlovic S, Roy I, St. Laurent M, Trypaluk C, Unruh D, Yekta M, Bonnin G (2013) 'NOAA Atlas 14, Volume 8 Version 2, precipitation-frequency atlas of the United States, Midwestern States.' (Silver Spring, MD, USA).

Pierson FB, Williams CJ (2016) Ecohydrologic impacts of rangeland fire on runoff and erosion: a literature synthesis. USDA Forest Service, Rocky Mountain Research Station, General Technical Report RMRS-GTR-351. (Fort Collins, CO, USA)

Pietraszek JH (2006) Controls on post-fire erosion at the hillslope scale, Colorado Front Range. MS Thesis. Colorado State University. (Fort Collins, CO, USA)

Price O, Bradstock R (2013) Landscape scale influences of forest area and housing density on house loss in the 2009 Victorian bushfires. *PLoS ONE* **8(8)**, e73421. doi:10.1371/journal.pone.0073421

R Core Team (2019) R: A language and environment for statistical computing. R Foundation for Statistical Computing, Vienna, Austria. URL https://www.R-project.org/.

Reinhardt ED, Keane RE, Calkin DE, Cohen JD (2008) Objectives and considerations for wildland fuel treatment in forested ecosystems of the interior western United States. *Forest Ecology and Management* **256**, 1997–2006. doi:10.1016/j.foreco.2008.09.016

Renard KG, Foster GR, Weesies GA, McCool DK, Yoder DC (1997) Predicting soil erosion by water: a guide to conservation planning with the Revised Universal Soil Loss Equation (RUSLE). USDA Agricultural Research Service Agricultural Handbook no. 703. (Washington, DC, USA)

Rengers FK, Tucker GE, Moody JA, Ebel BA (2016) Illuminating wildfire erosion and deposition patterns with repeat terrestrial lidar. *Journal of Geophysical Research: Earth Surface* **121**, 588-608. doi:10.1002/2015JF003600

Robichaud PR, Wagenbrenner JW, Brown RE, Wohlgemuth PM, Beyers JL (2008) Evaluating the effectiveness of contour-felled log erosion barriers as a post-fire runoff and erosion mitigation treatment in the western United States. *International Journal of Wildland Fire* **17**, 255–273. doi:10.1071/WF07032

Robichaud PR, Lewis SA, Wagenbrenner JW, Ashmun LE, Brown RE (2013a) Post-fire mulching for runoff and erosion mitigation. Part I: effectiveness at reducing hillslope erosion rates. *Catena* **105**, 75–92. doi:10.1016/j.catena.2012.11.015

Robichaud PR, Wagenbrenner JW, Lewis SA, Ashmun LE, Brown RE, Wohlgemuth PM (2013b) Post-fire mulching for runoff and erosion mitigation. Part II: effectiveness in reducing runoff and sediment yields from small catchments. *Catena* **105**, 93–111. doi:10.1016/j.catena.2012.11.016

Ryan SE, Dwire KA, Dixon MK (2011) Impacts of wildfire on runoff and sediment loads at Little Granite Creek, western Wyoming. *Geomorphology* **129**, 113–130. doi:10.1016/j.geomorph.2011.01.017

Schmeer SR (2014) Post-fire erosion response and recovery, High Park Fire, Colorado. MS Thesis. Colorado State University. (Fort Collins, CO, USA)

Schmeer SR, Kampf SK, MacDonald LH, Hewitt J, Wilson C (2018) Empirical models of annual post-fire erosion on mulched and unmulched hillslopes. *Catena* **163**, 276–287. doi:10.1016/j.catena.2017.12.029

Scott JH, Burgan RE (2005) Standard fire behavior fuel models: a comprehensive set for use with Rothermel's surface fire spread model. USDA Forest Service, Rocky Mountain Research Station, General Technical Report RMRS-GTR-153. (Fort Collins, CO, USA)

Scott JH, Reinhardt ED (2001) Assessing crown fire potential by linking models of surface and crown fire behavior. USDA Forest Service, Rocky Mountain Research Station, General Technical Research Paper RMRS-RP-29. (Fort Collins, CO, USA)

Scott JH, Thompson MP, Calkin DE (2013) A wildfire risk assessment framework for land and resource management. USDA Forest Service, Rocky Mountain Research Station, General Technical Report RMRS-GTR-315. (Fort Collins, CO, USA)

Shakesby RA, Doerr SH (2006) Wildfire as a hydrological and geomorphological agent. *Earth-Science Reviews* **74**, 269–307. doi:10.1016/j.earscirev.2005.10.006

Shakesby RA, Moody JA, Martin DA, Robichaud PR (2016) Synthesising empirical results to improve predictions of post-wildfire runoff and erosion response. *International Journal of Wildland Fire* **25**, 257-261. doi:10.1071/WF16021

Short KC, Finney MA, Vogler KC, Scott JH, Gilbertson-Day JW, Grenfell IC (2020) Spatial datasets of probabilistic wildfire risk components for the United States (270m). 2nd edition. USDA Forest Service Research Data Archive. (Fort Collins, CO, USA) doi:10.2737/RDS-2016-0034-2

Stephens SL, Moghaddas JJ (2005) Experimental fuel treatment impacts on forest structure, potential fire behavior, and predicted tree mortality in a California mixed- conifer forest. *Forest Ecology and Management* **215**, 21–36. doi:10.1016/j.foreco.2005.03.070

Stephens SL, Moghaddas JJ, Edminster C, Fielder CE, Haase S, Harrington M, Keeley JE, Knapp EE, McIver JD, Metlen K, Skinner CN, Youngblood A (2009) Fire treatment effects on vegetation structure, fuels, and potential fire severity in western U.S. forests. *Ecological Applications* **19**, 305–320. doi:10.1890/07-1755.1

Syphard AD, Rustigian-Romsos H, Mann M, Conlisk E, Moritz MA, Ackerly D (2019). The relative influence of climate and housing development on current and projected future fire patterns and structure loss across three California landscapes. *Global Environmental Change* **56**, 41-55. doi:10.1016/j.gloenvcha.2019.03.007

Theobald DM, Merritt DM, Norman JB (2010) Assessment of threats to riparian ecosystems in the western U.S. Report to the Western Environmental Threats Assessment Center, Prineville, OR by the USDA Stream Systems Technology Center and Colorado State University. (Fort Collins, CO, USA)

Thompson MP, Vaillant NM, Haas JR, Gebert KM, Stockmann KD (2013) Quantifying the potential impacts of fuel treatments on wildfire suppression costs. *Journal of Forestry* **111**, 49–58. doi:10.5849/jof.12-027

Tillery AC, Haas JR, Miller LW, Scott JH, Thompson MP (2014) Potential post-wildfire debris-flow hazards - a pre-wildfire evaluation for the Sandia and Manzano Mountains and surrounding areas, central New Mexico. US Geological Survey Scientific Investigations Report 2014–5161. (Albuquerque, NM, USA)

Tinkham WT, Hoffman CM, Ex SA, Battaglia MA, Saralecos JD (2016) Ponderosa pine forest restoration treatment longevity: implications of regeneration on fire hazard. *Forests* **7**, 137. doi:10.3390/f7070137

Toy TJ, Foster GR (1998) Guidelines for the use of the Revised Universal Soil Loss Equation (RUSLE) version 1.06 on mined lands, construction sites, and reclaimed lands. Office of Surface Mining and Reclamation (OSM), Western Regional Coordinating Center. (Denver, CO, USA)

US Census Bureau (2015) 2010 Census tract-level housing cost data. Available at https://www.census.gov/en.html

US Environmental Protection Agency (USEPA) and the US Geological Survey (USGS) (2012) National Hydrography Dataset Plus - NHDPlus. Version 2.1. Available online at: http://www.horizon-systems.com/NHDPlus/index.php

Wagenbrenner JW, MacDonald LH, Rough D (2006) Effectiveness of three post-fire rehabilitation treatments in the Colorado Front Range. *Hydrological Processes* **20**, 2989–3006. doi:10.1002/hyp.6146

Wagenbrenner JW, Robichaud PR (2014) Post-fire bedload sediment delivery across spatial scales in the interior western United States. *Earth Surface Processes and Landforms* **39**, 865–876. doi:10.1002/esp.3488

Walling DE (1983) The sediment delivery problem. *Journal of Hydrology* **65**, 209–237. doi:10.1016/0022-1694(83)90217-2

Wilson C, Kampf SK, Wagenbrenner JW, MacDonald LH (2018) Rainfall thresholds for post-fire runoff and sediment delivery from plot to watershed scales. *Forest Ecology and Management* **430**, 346–356. doi:10.1016/j.foreco.2018.08.025

Winchell MF, Jackson SH, Wadley AM, Srinivasan R (2008) Extension and validation of a geographic information system-based method for calculating the Revised Universal Soil Loss Equation length-slope factor for erosion risk assessments in large watersheds. *Journal of Soil and Water Conservation* **63**, 105–111. doi:10.2489/jswc.63.3.105

Wohl E (2013) Migration of channel heads following wildfire in the Colorado Front Range, USA. *Earth Surface Processes and Landforms* **38**, 1049–1053. doi:10.1002/esp.3429

Yang D, Kanae S, Oki T, Koike T, Musiake K (2003) Global potential soil erosion with reference to land use and climate changes. *Hydrological Processes* **17**, 2913–2928. doi:10.1002/hyp.1441

Yochum SE, Norman J (2014) West Fork Complex Fire: potential increase in flooding and erosion. USDA Natural Resources Conservation Service Report. (Denver, CO, USA)

Ziegler JP, Hoffman C, Battaglia M, Mell W (2017) Spatially explicit measurements of forest structure and fire behavior following restoration treatments in dry forests. *Forest Ecology and Management* **386**, 1-12. doi:10.1016/j.foreco.2016.12.002

## Appendix I: Water Supply Risk Assessment Details

The water supply risk assessment combines modeled fire likelihood and intensity with an effects analysis that includes predictions of post-fire erosion and sediment transport to water supplies and a translation to monetary impact using the stakeholder defined sediment impact costs (Figure 2). Fire likelihood is quantified with burn probability modeled with the large fire simulator (FSim; Finney et al. 2011) from Short et al. (2020). Fire intensity is accounted for using crown fire activity predicted with FlamMap 5.0 (Finney et al. 2015). Post-fire erosion is quantified for median rainfall conditions using a GIS-implementation of the Revised Universal Soil Loss Equation (RUSLE; Renard et al. 2015) by modifying the cover and soil erodibility factors. Sediment Delivery Ratio (SDR) models for hillslopes and channels (Wagenbrenner and Robichaud 2014; Frickel et al. 1975) were adapted to the planning area to estimate sediment transport to water supplies. The conditional and expected mass of sediment delivered to each water supply are then combined with sediment impact costs to quantify the conditional monetary impacts and risk to water supplies.

### Fire likelihood

Burn probability comes from a separate effort to estimate probabilistic wildfire hazard components with FSim (Short et al. 2020). FSim (Finney et al. 2011) models large fire occurrence, growth, and containment over many future fire seasons. Daily large fire occurrence is determined as a function of an artificial time series of the National Fire Danger Rating System Energy Release Component (ERC) for fuel model G calibrated with time series analysis of historical weather data. Fire growth is modeled using the minimum travel time algorithm (Finney 2002) based on topography and fuel conditions circa 2014 (LANDFIRE 2016), and daily fuel moisture, wind speed, and wind direction. Daily wind speed and direction are drawn randomly from their historical joint probability distribution by month. Fire containment is modeled based on primary fuel type and daily fire growth metrics (Finney et al. 2009). Short et al. (2020) calibrated FSim to approximate the historical fire size distribution and rate of burning within biophysical regions, called "pyromes", which have similar controls on wildfire activity. They distribute an estimate of burn probability at 270-m resolution calculated as the number of times each pixel burned over the 10,000 simulated fire seasons.

Two modifications are made to the FSim burn probability for use in the WIT. First, the raster is reprojected and resampled to 30-m resolution with bilinear interpolation to match the other raster products used in the analysis. Second, the annual burn probability estimate from FSim is adjusted to fuel treatment planning period burn probability given the focus on estimating the risk reduction potential of fuel treatments. The WIT makes the simplifying assumption that fuel treatments will have constant effectiveness for a period of 25 years based on projected recovery in crowning and torching indices (Tinkham et al. 2016) with the level of regeneration that is typical after forest restoration treatments in the Colorado Front Range (Francis et al. 2018). A shorter planning period is recommended for more

productive regions. Equation 1 is used to convert from the annual burn probability to burn probability over a 25-year period.

$$BP_{25} = 1 - (1 - BP_1)^{25} \qquad \textbf{Equation 1}$$

It is important to acknowledge the limitations of modeled burn probability. Burn probability modeling is akin to characterizing historical fire regimes in that it both seek to summarize general trends in the frequency of burning across a landscape instead of describing the exact extent and timing of wildfire activity. Burn probability modeling methods have evolved quickly since their introduction in the early 2000s and it is expected that new models and calibration techniques will continue to develop and improve our understanding of fire likelihood. The reader is referred to Finney et al. (2011) and Short et al. (2020) for discussion of limitations with the FSim model and its application to the modeling in this study. The recent review from Parisien et al. (2019) provides a general summary of burn probability modeling with relevant discussion of the unresolved need to validate predictions and debate about appropriate methods to do so. The consensus is that burn probability modeling can capture the relative trends in fire activity across a landscape given that the driving factors – ignition sources, climate, and fuels – do not appreciably change, but it is acknowledged that near-term patterns of fire activity are likely to vary from predictions, especially in systems where much of the fire activity occurs in infrequent, but large wildfires.

Fire likelihood is considered static in the WIT assessment of risk and risk reduction benefit (Figure 2) for three reasons. First, the WIT makes use of a nationally consistent data product that represents only baseline conditions (Short et al. 2020). Second, it is currently computationally infeasible to evaluate change in burn probability for each decision unit in the optimization model and how the prior decisions change the benefit of subsequent decisions. Incorporating treatment effects on burn probability into the optimization model would require serious approximations that largely negate the benefit of adding detailed modeling. Third, there is not currently a strong scientific consensus that fuel treatments will reduce burn probability without understanding if and how they may contribute to fire containment efforts (Agee et al. 2000; Reinhardt et al. 2008). FSim's current containment model (Finney et al. 2009) only addresses active suppression indirectly via the weather and growth conditions that facilitate containment. The most relevant estimate of fuel treatment effects on burn probability for the Peaks to People focus area comes from a study of large landscape fuel treatments in Oregon using pre- and post-treatment comparisons of fire activity modeled with FSim (Thompson et al. 2013). This study estimated that burn probability would be reduced by approximately 36% within the treated areas, but this effect diminished to 23% when considering areas within 2 miles of treatments, and to only 11% across the full landscape. It is reasonable to think that similar effects could be achieved in Northern Colorado with combined thinning and prescribed fire treatments.

**Fire behavior**

The FlamMap 5.0 spatial fire modeling system (Finney et al. 2015) is used to predict crown fire activity (CFA; Scott and Reinhardt 2001) as a proxy for soil burn severity. CFA is a

prediction of fire type in categories of unburned, surface fire, passive crown fire, and active crown fire. Surface fires spread primarily through live and dead fuels on the forest floor including litter, duff, wood, grass, and shrubs. Passive crown fires spread primarily through surface fuels but with sufficient intensity to initiate crown fire in patches of trees (also called "torching"). Active crown fire includes a substantial component of fire spread through the forest canopy (also called "crowning"). Surface fire intensity increases along the spectrum of surface to active crown fire behavior, so CFA is commonly used as a proxy for burn severity in watershed risk assessments by mapping surface, passive crown, and active crown fire to low, moderate, and high burn severity, respectively (Tillery et al. 2014; Haas et al. 2017; Jones et al. 2017).

FlamMap predicts CFA using spatial data on fuels and topography and specified fuel moisture and wind conditions. Baseline conditions are described in the assessment using circa 2016 raster fuels and topography data from LANDFIRE (2019). Canopy base height was reduced 30% and the fire behavior fuel model was changed to high load conifer litter (Scott and Burgan 2005) to reflect recent observations of extreme fire behavior in lodgepole pine forests (Moriarty et al. 2019). To represent current conditions (e.g. year 2020), fuels were also updated based on spatial fuel treatment and wildfire datasets from the USDA Forest Service, DOI National Park Service, the Colorado State Forest Service, Larimer County, and Peaks to People. Additionally, fuels were converted to open water for in progress and planned reservoirs.

Historical data from the Redfeather, Estes Park, and Redstone Remote Automated Weather Stations (RAWS) were used to identify an appropriate problem scenario for fire behavior modeling. Most area burns in the Colorado Front Range during very dry and windy conditions (Graham 2003), so the historical 97$^{th}$ percentile (extreme) weather conditions are used to represent the likely burning conditions. FireFamilyPlus 4.1 (Bradshaw and McCormick 2000) was used to summarize 25$^{th}$, 50$^{th}$, 90$^{th}$, and 97$^{th}$ percentile fire season (1 April to 31 October) conditions (Table 8). Wind speeds were converted from 10-minute averages to 1-minute averages to better reflect potential fire behavior (Crosby and Chandler 1966). Fuel moisture conditions were averaged across the three stations, but only the Redfeather and Estes Park stations were used for wind speed because Redstone is influenced heavily by upcanyon winds. The uphill wind direction option is used in FlamMap to model the worst case for each pixel.

*Table 8: Percentiles of fuel moisture by class and wind speeds from local RAWS. The 97$^{th}$ percentile conditions are used in the WIT analysis. Other percentiles are provided for comparison.*

| | Fuel moisture (%) | | | | | Wind speed (mph @ 20ft) | |
|---|---|---|---|---|---|---|---|
| **Percentile** | **1-hr** | **10-hr** | **100-hr** | **Herbaceous** | **Woody** | **10-min ave.** | **1-min ave.** |
| 25th | 8 | 10 | 14 | 58 | 94 | 5 | 9 |
| 50th | 5 | 7 | 11 | 33 | 63 | 7 | 11 |
| 90th | 3 | 4 | 7 | 4 | 63 | 12 | 17 |
| 97th | 2 | 3 | 6 | 2 | 63 | 15 | 20 |

It is important to acknowledge that fire behavior prediction systems, including FlamMap, were not designed to predict fire severity. There remains a need for basic research on the fire behavior metrics, observed or modeled, that best predict burn severity (Moody et al. 2013; Shakesby et al. 2016). CFA is a reasonable but likely imperfect proxy for burn severity because of the variety of surface and canopy fuel configurations that support crown fire behavior. Imperfect data and model accuracy also create uncertainty in fire behavior predictions. Fuel moisture and fire weather conditions are dynamic in space and time, so 97$^{th}$ percentile conditions will not match all future fire conditions. This is especially true for wind direction, which was assumed to blow upslope in this analysis to predict a consistently worst-case outcome across aspects. In reality, some aspects will be exposed to wind, while others will be shadowed. It is difficult to predict whether fire will be spreading up or down a slope without information on ignition location and wind direction. This analysis also does not account for terrain-influenced winds, which can cause wind to accelerate beyond the domain-averaged wind speeds used in the analysis. The pre-modeled burn severity should be viewed as representing the general tendency in burn severity based on fuels and topography.

**Hillslope Erosion**

The Revised Universal Soil Loss Equation (RUSLE) predicts annual soil loss (A) in Mg ha$^{-1}$ yr$^{-1}$ as the product of five sub-factors (Eqn 2): rainfall erosivity (R), soil erodibility (K), length and slope (LS), cover (C), and support practices (P) (Renard et al. 1997).

$$A = R \times K \times LS \times C \times P \qquad \textbf{Equation 2}$$

Spatial data and analyses are used to approximate the R, K, LS, and C factors for unburned conditions, as described in Theobald et al. (2010), Litschert et al. (2014), and Gannon et al. (2019), at 30-m resolution. Support practices (P), which typically refer to erosion mitigation actions, are not quantified in the assessment to model the unmitigated erosion hazard.

*Rainfall Erosivity*

Rainfall erosivity (R), also called "rainfall-runoff erosivity", is an annual metric of rainfall calculated as the product of total storm energy and maximum 30-minute intensity (MJ mm ha$^{-1}$ hr$^{-1}$). It is a better predictor of erosion magnitude than either rainfall depth or intensity alone, because it accounts for the available energy to detach soil particles and the occurrence of infiltration-excess overland flow to transport mobilized sediment (Renard et al. 1997). Rainfall erosivity was characterized using National Oceanic and Atmospheric Administration (NOAA) 15-minute rainfall data (Perica et al. 2013) from 11 rainfall stations representative of the Colorado Front Range climate that were assembled for a separate study (Wilson et al. 2018) and processed with the Rainfall Intensity Summarization Tool (RIST; Dabney 2016) to calculate storm-level rainfall erosivity. Storm-level rainfall erosivity was summed by year to calculate annual rainfall erosivity for each station and year. This data set spans the years 1971 to 2010 and includes 403 station-years of annual rainfall erosivity observations.

Rainfall erosivity is highly variable across space and time in the Colorado Front Range (Figure 17). We therefore treat rainfall as a random process described by the annual rainfall erosivity observations pooled across stations. Burned watersheds are most-susceptible to erosion for the first three years following wildfire (Benavides-Solorio and MacDonald 2005; Wagenbrenner et al. 2006; Robichaud et al. 2013a), so the WIT focuses on the total sediment production during these years. Exposure to post-fire rainfall erosivity is therefore most appropriately characterized by the distribution of three-year block means of annual rainfall erosivity. However, the annual and three-year erosivity distributions are not substantially different (Figure 18), so the annual distribution is used in the WIT for ease of interpretation. In the risk assessment, R is modeled as a spatially invariant surface of median annual rainfall erosivity (615 MJ mm $ha^{-1}$ $hr^{-1}$), which means R has no influence on the spatial variability in risk. Uncertainty in erosion-related risks is communicated in the performance metrics (see Appendix III) using the $5^{th}$ and $95^{th}$ percentiles of annual rainfall erosivity – 210 and 2300 MJ mm $ha^{-1}$ $hr^{-1}$ – to estimate an empirical 90% confidence interval for the predictions.

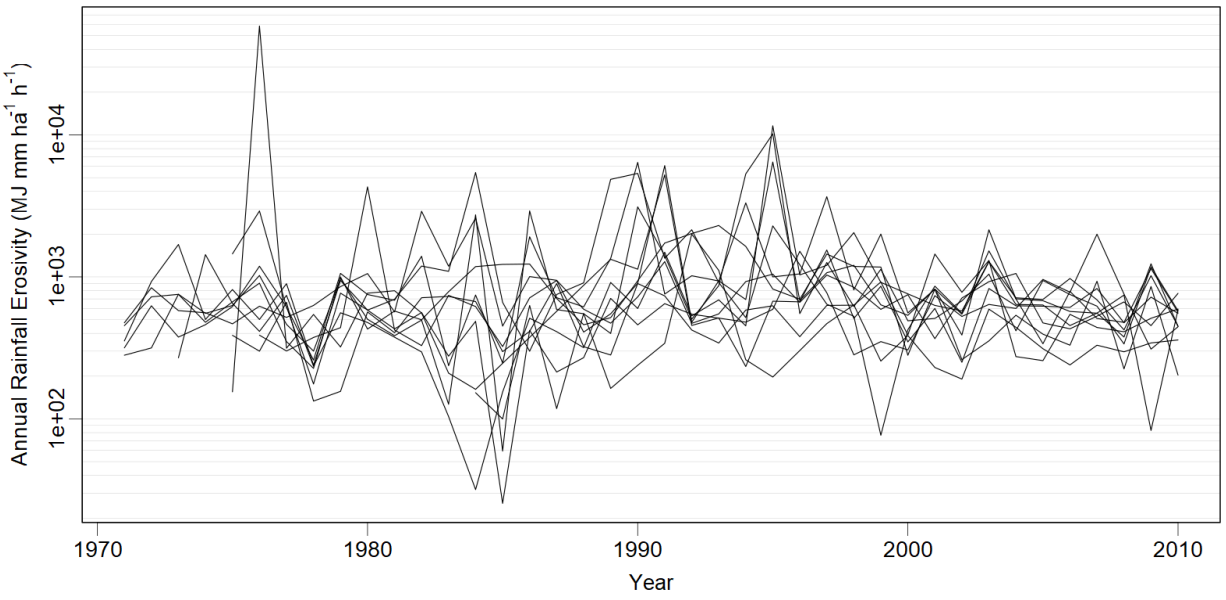


*Figure 17: Time series of rainfall erosivity for the eleven stations used in the analysis. Note log-scale y-axis.*

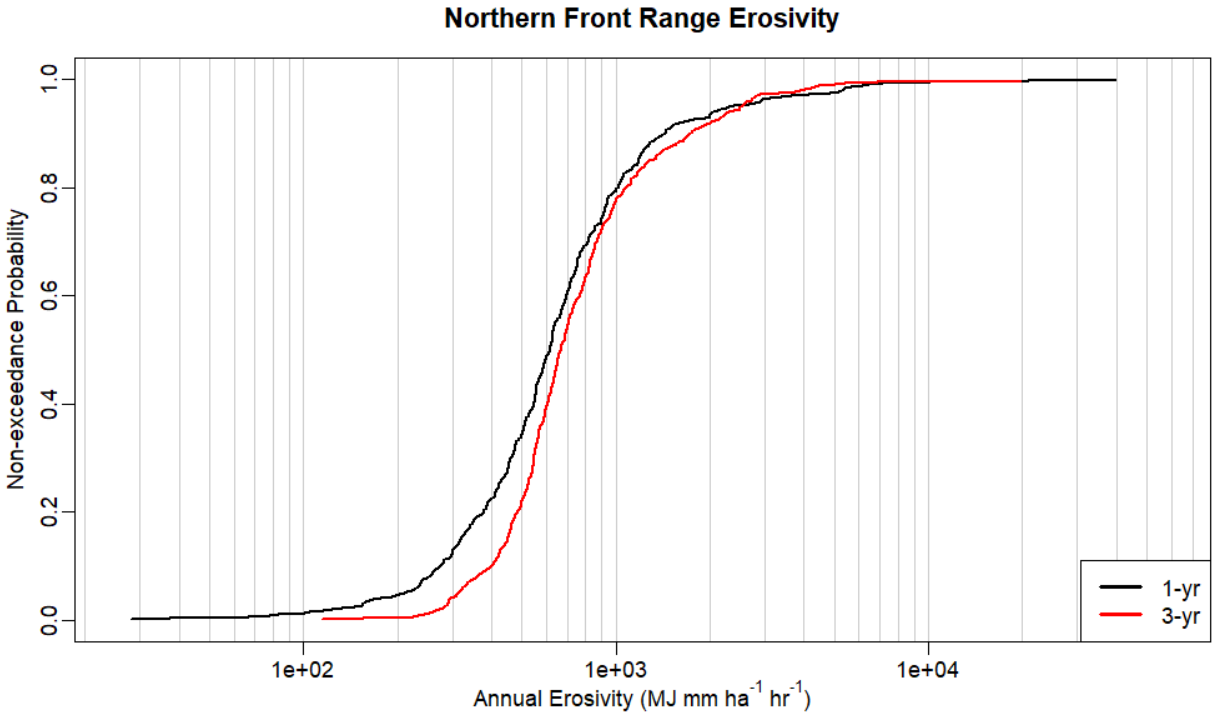


*Figure 18: Empirical cumulative frequency distribution of Colorado Front Range annual erosivity from 403 station-years of annual erosivity observations. The one-year block distribution is used in the WIT.*

*Soil Erodibility*

Undisturbed soil erodibility (K) is described using the Soil Survey Geographic Database (SSURGO) gap-filled where necessary with the State Soil Geographic Database (STATSGO) (NRCS Soil Survey Staff 2016). The procedures of Yochum and Norman (2014) are used to calculate a weighted mean of whole soil K factor (Kwfact) for each map unit. First, the component depth-weighted mean K is calculated for the top 15 cm of soil. Then the map unit area-weighted mean K is calculated based on the proportional coverage of components. Components mapped as rock do not have K values assigned to them, but complete bedrock coverage is rare within these map units based on inspection of aerial imagery. Instead of treating rock components as zero K, they are assigned 20% of the area-weighted mean K of the other components in the same map unit. SSURGO map units that are missing K values for more than 50% of their area are gap-filled with equivalent metrics from STATSGO. All K values are converted to metric units (Renard et al. 1997).

*Length and Slope*

The combined length and slope (LS) factors are calculated using terrain analysis of a 30-m DEM (USEPA and USGS 2012) following methods in Theobald et al. (2010). The slope portion (S) is calculated per Nearing (1997) where θ is slope steepness in radians (Eqn 3). Consistent with previous studies (Theobald et al. 2010; Litschert et al. 2014), θ is limited to 55% when calculating S to not extrapolate beyond the range of Nearing's data.

$$S = -1.5 + \frac{17}{1 + e^{(2.3 - 6.1 \times \sin\theta)}}$$ **Equation 3**

LS is then calculated per Winchell et al. (2008) where $A$ is the contributing area to the cell inlet in m$^2$, $D$ is the cell dimension in m, $m$ is slope-length exponent, and $x$ is the shape factor calculated as a function of cell aspect (α) in radians (Eqns 4-7). The slope-length exponent ($m$) is based on the ratio of rill to interrill erosion (β), which is estimated from slope steepness (θ) based on McCool et al. (1989).

$$LS = S \times \frac{(A + D^2)^{m+1} - A^{m+1}}{D^{m+2} \times x^m \times 22.13^m}$$ **Equation 4**

$$m = \frac{\beta}{1 + \beta}$$ **Equation 5**

$$\beta = \frac{\frac{sin\theta}{0.0896}}{3 \times sin\theta^{0.8} + 0.56}$$ **Equation 6**

$$x = |sin\alpha| + |cos\alpha|$$ **Equation 7**

Slope steepness (θ), slope aspect (α), and contributing area ($A$) are calculated from a 30-m resolution filled DEM using standard slope, aspect, and D8 flow direction methods in ArcGIS 10.3. When calculating LS, $A$ is limited to 3,000 m$^2$ to approximate the maximum hillslope length of 300 m suggested in Renard et al. (1997). LS values are also constrained to the maximum of 72.15 from Renard et al. (1997).

*Cover*

Undisturbed cover factors (C) are assigned by mapping an appropriate C reported in previous studies (Table 9) to each Existing Vegetation Type (EVT) from LANDFIRE (2016). The lowest values of C are assigned to forests (low erosion), moderate values are assigned to sparse grass and shrub cover types, and the highest values are assigned to cover types associated with agriculture or mining. We assigned sparsely vegetated but rocky cover types a C of 0.002 because these environments should be minimally impacted by fire (e.g., alpine bedrock and scree).

*Table 9: Cover factor (C) values (unitless) from previous studies are assigned to LANDFIRE Existing Vegetation Type (EVT) (2016). The top 30 vegetation types, which account for >95% of the area, are shown here.*

| EVT class name | % of Area | C factor | Reference |
|---|---|---|---|
| Southern Rocky Mountain Ponderosa Pine Woodland | 20.0 | 0.0027 | Miller et al. 2003 |
| Rocky Mountain Lodgepole Pine Forest | 18.0 | 0.002 | Breiby 2006 |
| Rocky Mountain Subalpine Dry-Mesic Spruce-Fir Forest and Woodland | 11.0 | 0.002 | Breiby 2006 |
| Western Great Plains Foothill and Piedmont Grassland | 7.0 | 0.012 | Breiby 2006 |
| Rocky Mountain Lower Montane-Foothill Shrubland | 6.7 | 0.025 | Breiby 2006 |
| Southern Rocky Mountain Montane-Subalpine Grassland | 5.8 | 0.012 | Breiby 2006 |
| Southern Rocky Mountain Dry-Mesic Montane Mixed Conifer Forest and Woodland | 3.7 | 0.002 | Breiby 2006 |
| North American Glacier and Ice Field | 2.5 | 0.001 | Yang et al. 2003 |
| Inter-Mountain Basins Montane Sagebrush Steppe | 2.3 | 0.029 | McCuen 1998 |
| Rocky Mountain Alpine Bedrock and Scree | 1.9 | 0.002 | Professional opinion |
| Recently Burned-Shrub Cover | 1.7 | 0.0348 | McCuen 1998 |
| Recently Burned-Tree Cover | 1.6 | 0.01 | Larsen and MacDonald 2007 |
| Interior Western North American Temperate Ruderal Grassland | 1.3 | 0.012 | Breiby 2006 |
| Rocky Mountain Aspen Forest and Woodland | 1.1 | 0.001 | Breiby 2006 |
| Rocky Mountain Alpine Turf | 1.1 | 0.012 | Breiby 2006 |
| Open Water | 0.9 | 0 | Breiby 2006; McCuen 1998 |
| Rocky Mountain Alpine-Montane Wet Meadow | 0.9 | 0.001 | Breiby 2006 |
| Western Cool Temperate Pasture and Hayland | 0.8 | 0.14 | McCuen 1998 |
| Developed-Roads | 0.8 | 0.0001 | Toy and Foster 1998 |
| Western Great Plains Shortgrass Prairie | 0.8 | 0.08 | Yang et al. 2003 |
| Recently Burned-Herb and Grass Cover | 0.7 | 0.0144 | Breiby 2006 |
| Western Cool Temperate Developed Ruderal Grassland | 0.7 | 0.012 | Breiby 2006 |
| Western Cool Temperate Developed Ruderal Evergreen Forest | 0.6 | 0.004 | Fu et al. 2006 |
| Southern Rocky Mountain Ponderosa Pine Savanna | 0.6 | 0.0027 | Miller et al. 2003 |
| Southern Rocky Mountain Mesic Montane Mixed Conifer Forest and Woodland | 0.6 | 0.002 | Breiby 2006 |
| Rocky Mountain Lower Montane-Foothill Riparian Woodland | 0.6 | 0.01 | Breiby 2006 |
| Developed-Low Intensity | 0.5 | 0.002 | Fu et al. 2006 |
| Rocky Mountain Cliff Canyon and Massive Bedrock | 0.4 | 0.002 | Professional opinion |
| Rocky Mountain Subalpine-Montane Limber-Bristlecone Pine Woodland | 0.4 | 0.002 | Breiby 2006 |
| Western Cool Temperate Developed Ruderal Shrubland | 0.4 | 0.029 | McCuen 1998 |

### *Fire Effects on Erosion*

Fire-related increases in erosion are primarily attributed to changes in surface cover (Larsen et al. 2009) and altered soil properties (Shakesby and Doerr 2006); therefore, fire effects on erosion are modeled by modifying the RUSLE C and K factors. For forests (≥ 10% canopy cover as mapped by LANDFIRE [2016]), post-fire C is changed to the mean first-year post-fire C factors by burn severity reported in Larsen and MacDonald (2007) (Table 10). Due to the diversity of non-forested vegetation types (< 10% canopy cover) and the limited estimates of fire effects in these systems (Pierson and Williams 2016), proportional adjustment factors are used to model fire effects on C (Table 10). Fire decreases soil infiltration capacity and cohesion owing to deposition of hydrophobic compounds, soil sealing, and consumption of organic material (DeBano et al. 2005; Shakesby and Doerr 2006). Direct measures of post-fire K factors are lacking, but Larsen and MacDonald (2007) back-calculated that K was increased by a factor of 2.5 for high burn severity. Given the limitations with their method of estimating change in K, more conservative adjustment factors are used to estimate fire effects on K (Table 10) like Schmeer (2014).

*Table 10: Mean post-fire C factor values by burn severity from Larsen and MacDonald (2007) are used to assign post-fire C for forests (≥ 10% LANDFIRE canopy cover). Fire effects on C factor for non-forest (< 10% LANDFIRE canopy cover) are applied as proportional adjustment factors. Fire effects on K factor for all vegetation are applied as proportional adjustment factors.*

| | | Fire Effects | | |
|---|---|---|---|---|
| **Crown Fire Activity** | **Burn Severity** | **Forest C** | **Non-forest C Adjustment Factor** | **K Adjustment Factor** |
| Surface | Low | 0.01 | 1.2 | 1.5 |
| Passive | Moderate | 0.05 | 1.5 | 1.75 |
| Active | High | 0.20 | 2.0 | 2.0 |

The WIT focuses on the increase in post-fire erosion by differencing the post-fire and pre-fire erosion predictions. RUSLE can predict very high erosion rates on the steepest slopes; although erosion potential may be this high, sediment availability will likely limit these high rates from being realized. Post-fire erosion increases are therefore limited to 200 Mg $ha^{-1}$ $yr^{-1}$ based on the maximum observed rates in the western US (Moody and Martin 2009). Hillslope erosion typically remains elevated for 2-5 years after fires in the Colorado Front Range (Benavides-Solorio and MacDonald 2005; Wagenbrenner et al. 2006; Robichaud et al. 2013a). To simplify, the WIT accounts for increased erosion for the first three years post-fire using a correction factor applied to the first-year predictions. We estimate that with constant rainfall, erosion in year two should be 15% lower than in year one and erosion in year three should be 75% less than year one, based on the rate of surface cover recovery and its influence on erosion (Pietraszek 2006; Benavides-Solorio and MacDonald 2005; Larsen et al. 2009). Therefore, we multiply the first-year post-fire erosion estimate by a factor of 2.1 to estimate the total post-fire sediment yield over the first three years.

The RUSLE model was originally developed for agricultural use (Renard et al. 1997) and the GIS implementation we use approximates the original model. The most significant departure from the original is the raster-based calculation of the LS factor, which has been validated for use in agricultural settings (Winchell et al. 2008), but not for use in mountainous terrain. The implementation used here controls for excessive erosion predictions on very steep, long slopes by limiting the S subfactor, flow accumulation values, combined LS factors, and resulting erosion predictions to the maximum values reported in previous studies. When pixel-level estimates of erosion are averaged to the catchment-level, most of the predicted sediment yields from hillslope erosion are within the range reported by previous studies (see Watershed Model Evaluation section). The baseline C factor values also have moderate uncertainty due to the use of best judgement to assign values from previous studies to remotely sensed landcover types. This uncertainty is greatest for the non-forest vegetation types because of the way fire effects are modeled with adjustment factors. The soils data are also fairly course and soil properties are sometimes inconsistent across areas that were surveyed at different times by different personnel. Spatial and temporal variability in annual rainfall erosivity spans several orders of magnitude, suggesting the actual post-fire erosion depends strongly on the subsequent rainfall, which cannot be predicted in advance. Erosion is modeled for median rainfall

erosivity in the WIT so impacts could be higher than predicted if fires are followed by more extreme rainfall.

**Hillslope Sediment Transport**

The proportion of hillslope sediment delivered to the stream channel network is estimated with an empirical model of post-fire hillslope sediment delivery ratio (*hSDR*) from the western US (Wagenbrenner and Robichaud 2014). *SDR* quantifies the proportion of gross erosion that is delivered to the outlet of a catchment. When hillslope erosion is the primary source of sediment, unit area sediment yields decline with increasing watershed size (*hSDR* < 1) because some sediment is stored on hillslopes and in channels (Walling 1983). First, the NHDPlus stream channel network is extended to include all pixels with greater than 10.8 ha contributing area (Henkle et al. 2011) because the flowline network does not include all channels and it especially underestimates the extent of the channel network after wildfire (Wohl 2013). The annual length ratio model from Wagenbrenner and Robichaud (2014) is then used to estimate post-fire *hSDR* (Eqn 8). Terrain analysis of a 30-m DEM (USEPA and USGS 2012) is used to calculate the flow path length from each pixel to the nearest stream channel as the "catchment length" and the flow path length across the pixel as the "plot length".

$$\log(hSDR) = -0.56 - 0.0094 * \left(\frac{Flow\ path\ length\ to\ nearest\ channel}{Flow\ path\ length\ across\ pixel}\right) \qquad \textbf{Equation 8}$$

The base predictions from this model suggest a maximum *hSDR* of only 0.27 for areas adjacent to streams, which is lower than what similar models based on travel time predict (Ferro and Porto 2000; Fernandez et al. 2003). As we show later in the Watershed Model Evaluation section, the base model also underpredicted catchment-level net sediment yields compared to field measurements in the region. Therefore, to roughly calibrate to local field observations, we double the predicted *hSDR* values, which produces a range of 0.09 to 0.54. Channels pixels are assigned *hSDR* of 1. Catchment-level sediment delivery to the draining flowline ($TS$) is calculated in Mg as the sumproduct of the pixel-level erosion ($A$) and *hSDR* values, indexed with $i$, and a correction factor to adjust for pixel size (Eqn 9).

$$TS = \sum_{i=1}^{N} A_i \times 0.09 \frac{ha}{pixel} \times hSDR_i \qquad \textbf{Equation 9}$$

*hSDR* is an approximation of highly dynamic sediment transport processes. The source of the model used here documents that substantial variability in *SDR* remains unexplained by their model and that some sites in Colorado do not fit the expected pattern of declining sediment yields with increasing catchment size (Wagenbrenner and Robichaud 2014). The *hSDR* model was developed from catchments burned mostly at moderate or high severity, so it could overestimate sediment yield from areas burned at low severity and burned areas separated from the stream by an unburned buffer. Although more sophisticated models are available for predicting sediment transport, they depend strongly on hydrologic conditions, which cannot be predicted in advance, or multi-scale sediment yield observations for calibration.

## Stream Channel Sediment Transport

The proportion of sediment transported to water supplies is estimated with a channel sediment delivery ratio (*cSDR*) model (Frickel *et al.* 1975) modified for the channel types in the study area. Low order channels in the study area are characterized by ephemeral or intermittent flow and high roughness from coarse bed material and streamside vegetation. The highest order channels are still steep mountain streams with considerably greater transport capacity due to higher magnitude perennial flows. Previous observations in this region suggest sediment transport efficiency should be very efficient in the highest order channels (Moody and Martin 2001; Miller et al. 2017), especially for silts and clays (Ryan et al. 2011). To approximate these trends, *cSDRs* of 0.75, 0.80, 0.85 and 0.95 per 10 km of stream length are assigned to 1st, 2nd, 3rd, and 4th or higher-order streams, respectively. Flowline *cSDR* is then calculated based on length per Eqn 10.

$$cSDR = cSDR_{10\ km}^{\left(\frac{Length\ in\ km}{10\ km}\right)} \quad \textbf{Equation 10}$$

Flowlines intercepting lakes and reservoirs are assigned a *cSDR* of 0.05 to reflect that most sediment will be trapped. The mass of fire-related sediment (Mg) delivered to a water supply ($TWS$) is calculated in Mg as the sum of sediment delivered to streams for all upstream catchments multiplied by the product of *cSDRs* for the intervening flowlines (Eqn 11).

$$TWS = \sum_{j=1}^{O}(TS_j \times \prod_{k=1}^{P} cSDR_k) \quad \textbf{Equation 11}$$

The subscript *j* is the index for the *O* upstream catchments and the subscript *k* is the index for the *P* intervening flowlines between catchment *j* and the water supply.

*cSDR* is also an approximation of highly dynamic sediment transport processes. Sediment transport in streams depends on the magnitude and timing of sediment and water inputs, which cannot be accurately predicted in advance, thus negating much of the benefit of advanced sediment transport models. The model used here approximates the trends in sediment transport efficiency documented in previous studies, but the use of stream order ignores within-order variability in flow, slope, and roughness that influence bedload transport rates.

## Watershed Model Evaluation

The post-fire erosion and sediment transport modeling used here has several limitations that are important to acknowledge. The linked erosion and sediment transport system is subject to multiple data, model, and model linkage uncertainties that have potential for prediction error, especially when coupled. The approximate calibrations made for erosion prediction in the Colorado Front Range may not be reasonable in other locations.

To evaluate model performance, we compared our modeled first year post-fire sediment yields to regional field observations at multiple scales of measurement (Figure 19). Most of our predicted first-year post-fire hillslope erosion rates at the catchment-level are close to the study-wide means of 9.5–22.2 Mg $ha^{-1}$ and the range of individual hillslope observations of 0.1–38.2 Mg $ha^{-1}$ from previous fires in the region exposed to moderate rainfall (Wagenbrenner et al. 2006; Larsen et al. 2009; Robichaud et al. 2013a; Schmeer et al. 2018). Few catchments are predicted to exceed the 72 Mg $ha^{-1}$ of rill and interrill erosion reported in the first year after the Buffalo Creek Fire in response to extreme rainfall (converted from Moody and Martin 2001 using a bulk density of 1.6 Mg $m^{-3}$). Despite doubling the efficiency of hillslope transport, fewer than half of all catchments approach the small catchment sediment yields from the Hayman Fire (Robichaud et al. 2008, 2013b). None of the catchments are predicted to deliver sediment to the pipeline in excess of the whole watershed sediment yield of 52.5 Mg $ha^{-1}$ for the first year of the Buffalo Creek Fire (Moody and Martin 2001).

Compared to these limited data points, the system of models makes reasonable sediment yield predictions, but it is unlikely that it perfectly represents the erosion and sediment transport processes. Some of our hillslope erosion predictions are higher than commonly observed values (Figure 19). This is likely due to a combination of factors. Some modeled catchments could have higher post-fire erosion potential than previously monitored areas. The use of contributing area in place of hillslope length in the spatial implementation of RUSLE (Winchell et al. 2008) means that convergent areas are predicted to have high erosion rates. Although this diverges from the original intent for RUSLE to be used on planar hillslopes, it matches observations of higher sediment yields in convergent areas that others sometimes report as drainage or channel erosion (Moody and Martin 2001; Pietraszek 2006; Rengers et al. 2016). Many of the hillslope erosion studies used for evaluation also had hillslope sediment fences fill and overtop, so the reported yields are usually interpreted as a lower bound estimate of the true erosion rate. For the hillslope transport component, it is possible that our rough calibration of the *hSDR* model to field observations could be mistaking higher yields from different erosion processes for efficient hillslope transport. Together, the RUSLE and *hSDR* model likely capture a mix of hillslope and channel erosion and sediment transport processes that could be better represented with spatially distributed models of the true processes. More observations of post-fire sediment yields from large watersheds are needed to further evaluate the channel transport component.

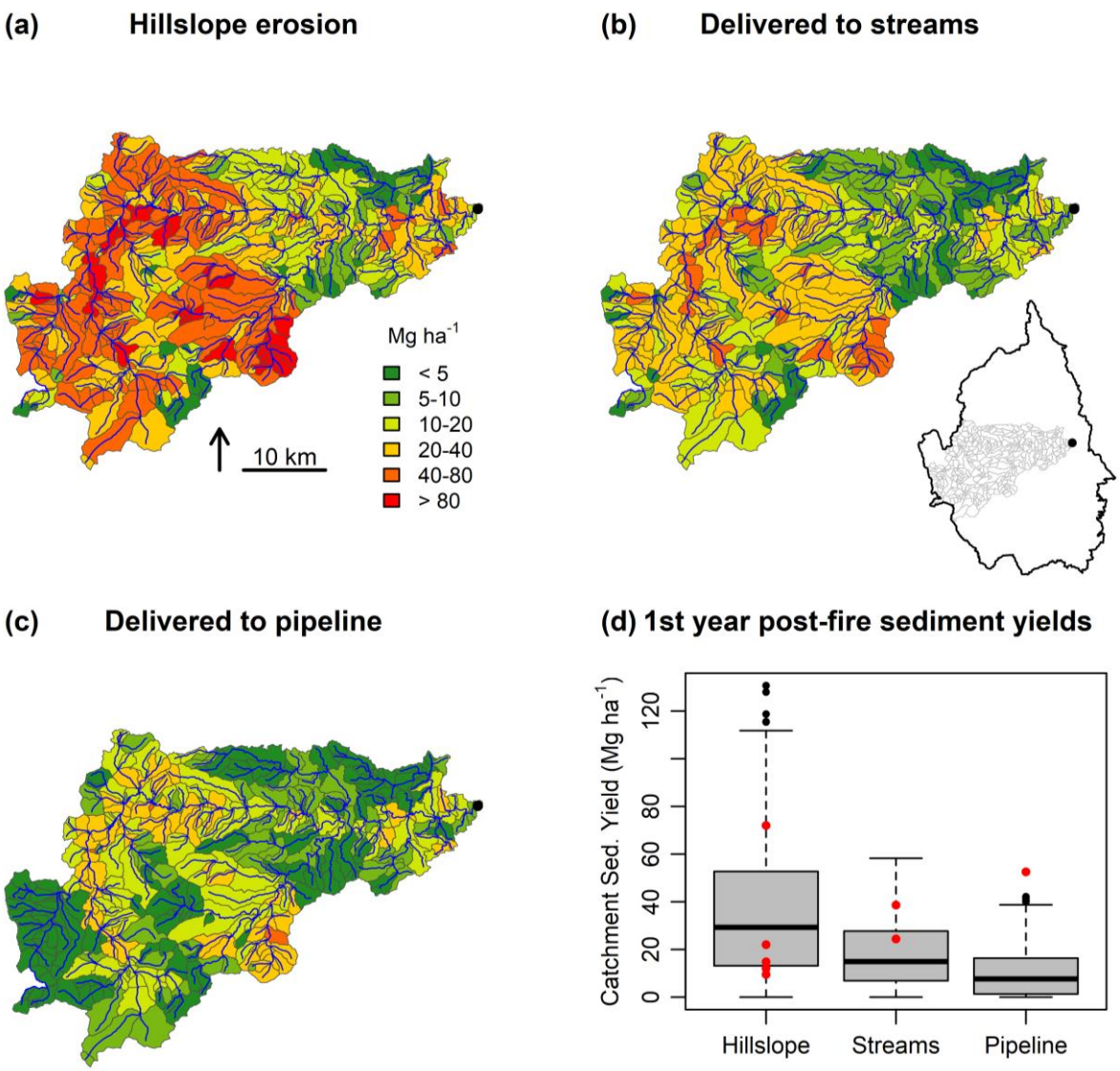


*Figure 19: Predicted first year mean post-fire sediment yields (Mg ha$^{-1}$) for each of the 435 catchments that contribute to a drinking water pipeline (a subset of the study area) for: (a) hillslope erosion; (b) sediment delivered to streams; and (c) sediment delivered to the pipeline. Catchment mean sediment yields decline from hillslope to whole watershed domains (d). Red dots in (d) are measured first-year mean post-fire sediment yields from Colorado field studies: hillslopes (Moody and Martin 2001; Wagenbrenner et al. 2006; Larsen et al. 2009; Robichaud et al. 2013a; Schmeer et al. 2018), small catchments (Robichaud et al. 2008, 2013b) and watershed (Moody and Martin 2001).*

# Appendix II: Fuel Treatment Optimization Details

## Linear program formulation

Objective function:

$$\max Z = \sum_{i=1}^{N}\sum_{t=1}^{P} RR_{i,t} * x_{i,t}$$

Constraints:

$$x_{i,t} \leq F_{i,t} \qquad \forall\, i,t$$

$$\sum_{t=1}^{P} x_{i,t} \leq tF_i \qquad \forall\, i$$

$$x_{i,t} \geq 0 \qquad \forall\, i,t$$

$$\sum_{i=1}^{N}\sum_{t=1}^{P} TC_{i,t} * x_{i,t} \leq Budget * BP_t \qquad \forall\, i,t$$

$$\sum_{i=1}^{N}\sum_{t=1}^{P} TC_{i,t} * x_{i,t} \leq Budget$$

Subscript notation:

$i$ is used to index treatment units from 1 to $N$

$t$ is used to index treatment types from 1 to $P$

Decision variables:

$x_{i,t}$ is the area (ac) of treatment $t$ assigned to treatment unit $i$

Parameters:

$Z$ is the total risk reduction (USD)

$RR_{i,t}$ is the risk reduction (USD ac$^{-1}$) for treatment $t$ applied to treatment unit $i$

$F_{i,t}$ is the feasible area (ac) for treatment $t$ in treatment unit $i$

$tF_i$ is the total feasible area (ac) for any treatment in treatment unit $i$

$TC_{i,t}$ is the cost (USD ac$^{-1}$) of applying treatment $t$ in treatment unit $i$

$Budget$ is the funding available for fuel treatment (USD)

$BP_t$ is the maximum budget proportion that can be allocated to treatment type $t$

Minimum and maximum treatment sizes (ac) are also imposed on the model by pre-processing decision units to eliminate those that fall under the minimum treatment size and by shrinking the feasible acres for those decision units that exceed the maximum treatment size.

## Treatment effects

Fuel treatment effects on risk are addressed in the assessment by altering the baseline fuels characteristics for the fire modeling and re-running the risk assessment for post-treatment conditions (Figure 2). Post-treatment risk is then subtracted from the baseline risk to estimate risk reduction as the benefit to be maximized in the optimization model.

The three treatments currently considered in the model for Northern Colorado are thinning, prescribed fire, and a complete treatment consisting of thinning followed by prescribed fire. The primary effects of treatments on the fuel variable inputs to FlamMap (Finney et al. 2015) are modeled with proportional adjustments for canopy variables (Table 11) and categorical changes in the fire behavior fuel model for surface fuels (Table 12) based on the mean effects of hazardous fuels reduction and forest restoration projects in the western U.S. (Stephens and Moghaddas 2005; Stephens et al. 2009; Fulé et al. 2012; Ziegler et al. 2017; Heinsch et al. 2018). These same effects are also used for updating the LANDFIRE (2019) fuels data to current conditions.

The canopy adjustments (Table 11) represent that thinning treatments reduce canopy cover and canopy bulk density (canopy fuel per volume) by removing trees. Thinning for restoration or hazardous fuels reduction typically targets the smallest trees for removal, which increases the average canopy base height and canopy height. Prescribed fire results in smaller changes to canopy fuels where it has been studied in California (Stephens and Moghaddas 2005). Initial monitoring of prescribed fire effects in Northern Colorado suggest it has more significant effects on canopy fuels than in California, likely due to the shorter stature of our forests (Morici et al. 2019). Future updates to the WIT may revise prescribed fire effects if this trend is confirmed by additional monitoring.

*Table 11: Proportional adjustment factors used to estimate treatment effects on canopy variables. CBD = canopy bulk density. CBH = canopy base height. CC = canopy cover. CH = canopy height.*

| | Adjustment factor | | | |
|---|---|---|---|---|
| **Treatment** | **CBD** | **CBH** | **CC** | **CH** |
| Thin | 0.60 | 1.20 | 0.70 | 1.20 |
| Rx fire | 0.92 | 1.09 | 0.95 | 1.13 |
| Complete | 0.50 | 1.20 | 0.75 | 1.20 |

*Table 12: Fire behavior fuel model changes by surface fuel management type using standard codes from Scott and Burgan (2005). Changes are highlighted in bold, red type.*

| Code | Baseline | Manage | Rx fire | Rearrange |
|---|---|---|---|---|
| NB1 | 91 | 91 | 91 | 91 |
| NB2 | 92 | 92 | 92 | 92 |
| NB3 | 93 | 93 | 93 | 93 |
| NB4 | 94 | 94 | 94 | 94 |
| NB5 | 95 | 95 | 95 | 95 |
| NB6 | 96 | 96 | 96 | 96 |
| NB7 | 97 | 97 | 97 | 97 |
| NB8 | 98 | 98 | 98 | 98 |
| NB9 | 99 | 99 | 99 | 99 |
| GR1 | 101 | 101 | 101 | **201** |
| GR2 | 102 | 102 | **101** | **201** |
| GR3 | 103 | 103 | **101** | **201** |
| GR4 | 104 | 104 | **101** | **201** |
| GR5 | 105 | 105 | **101** | **201** |
| GR6 | 106 | 106 | **101** | **201** |
| GR7 | 107 | 107 | **101** | **201** |
| GR8 | 108 | 108 | **101** | **201** |
| GR9 | 109 | 109 | **101** | **201** |
| GS1 | 121 | 121 | 121 | **201** |
| GS2 | 122 | 122 | **121** | **201** |
| GS3 | 123 | 123 | **121** | **201** |
| GS4 | 124 | 124 | **121** | **201** |
| SH1 | 141 | 141 | 141 | **201** |
| SH2 | 142 | 142 | **141** | **201** |
| SH3 | 143 | 143 | **141** | **201** |
| SH4 | 144 | 144 | **141** | **201** |
| SH5 | 145 | 145 | **141** | **201** |
| SH6 | 146 | 146 | **141** | **201** |
| SH7 | 147 | 147 | **141** | **201** |
| SH8 | 148 | 148 | **141** | **201** |
| SH9 | 149 | 149 | **141** | **201** |
| TU1 | 161 | 161 | 161 | **201** |
| TU2 | 162 | 162 | **161** | **201** |
| TU3 | 163 | 163 | **161** | **201** |
| TU4 | 164 | 164 | **161** | **201** |
| TU5 | 165 | 165 | **161** | **201** |
| TL1 | 181 | 181 | 181 | **201** |
| TL2 | 182 | 182 | **181** | **201** |
| TL3 | 183 | 183 | **181** | **201** |
| TL4 | 184 | 184 | **181** | **201** |
| TL5 | 185 | 185 | **181** | **201** |
| TL6 | 186 | 186 | **181** | **201** |
| TL7 | 187 | 187 | **181** | **201** |
| TL8 | 188 | 188 | **181** | **201** |
| TL9 | 189 | 189 | **181** | **201** |
| SB1 | 201 | 201 | 201 | 201 |
| SB2 | 202 | **201** | **201** | **201** |
| SB3 | 203 | **201** | **201** | **201** |
| SB4 | 204 | **201** | **201** | **201** |

Fire behavior fuel models (Scott and Burgan 2005) are widely used in fire modeling to represent common fuel types, loadings, and arrangements and their characteristic flame lengths (or intensities) and rates of spread. Because fire behavior fuel models are categorical with finite options (n=40 in Scott and Burgan 2005), they do not offer a high degree of precision to represent treatment effects. Most studies of fuel treatment effects in the western U.S. (Stephens and Moghaddas 2005; Stephens et al. 2009; Fulé et al. 2012) suggest surface fuels should increase slightly with thinning only treatments, but the amount, type, and arrangement of logging residues can vary widely based on harvesting methods. Initial monitoring of thinning treatments in Northern Colorado suggests the surface fuel additions are minor when the preferred method of mechanical whole-tree harvesting is used (Morici et al. 2019). Therefore, we assume some form of slash management will accompany thinning treatments, so the surface fuel additions will be minor enough that changing the fire behavior fuel model is not warranted (Table 12). The one exception is that we assume heavy standing and downed fuels in slash-blowdown fuel types would be addressed by treatment (Table 12). Prescribed fire effects are represented as changing the fire behavior fuel model to the least intense model in each fuel model type (e.g., *timber understory*, *timber litter*; Table 12). A *rearrange* surface fuel treatment is presented (Table 11) to describe lop and scatter and mastication effects on intensifying surface fire behavior based on the masticated fuel bed burning experiments of Heinsch et al. (2018). The rearrange option is not applied to any of the hypothetical future treatments; it is only used to represent some past actions when updating fuels data to reflect current conditions.

The methods used to represent the primary effects of treatments on fuels have some limitations. Foremost, they are dependent on LANDFIRE (2019) accurately representing the baseline fuel conditions. Modeling treatments with mean effects implies that the intensity of treatment is uniform, which is obviously difficult to attain with prescribed fire, and conflicts with restoration guidance for the region that advocates for intentionally creating heterogeneity in forest structure with thinning treatments (Addington et al. 2018). Fine-scale differences in treatment effects between the model and reality should not significantly affect the mean benefit of the treatment on a given unit of the landscape. Using fire behavior fuel model reclassifications to represent treatment effects on surface fuels is also an approximation of reality.

## Treatment feasibility

Treatment feasibility modeling focuses on mapping the hard constraints on treatment placement in a binary raster format (0 = infeasible; 1 = feasible). The spatial resolution and alignment of the rasters should match the LANDFIRE (2019) data used elsewhere in the WIT analyses.

*Thinning*

The thinning treatment is restricted to forested environments that do not have land designations precluding active management. Forested is defined as areas mapped by LANDFIRE (2019) with greater than or equal to 10% canopy cover. Land management designations precluding active management include USDA Forest Service wilderness, National Park Service wilderness, and Forest Service upper tier roadless. Within Rocky Mountain National Park, mechanical treatments are restricted to within 3 miles of the eastern park boundary based on the spatial distribution of past projects and the park's primary fire management objective to reduce wildfire transmission into communities.

*Prescribed fire*

Prescribed fire as a first-entry tool is restricted to dry forests associated with frequent to moderate fire return intervals and primarily low to mixed severity effects identified from the present LANDFIRE (2019) existing vegetation types (Table 13). Notably, this list does not include lodgepole pine or spruce-fir forest types. Prescribed fire is also limited from areas within 250 m of buildings as mapped by Caggiano et al. (2016).

*Table 13: LANDFIRE (2019) existing vegetation types considered appropriate for prescribed fire as a first-entry tool.*

| Value | Name |
|---|---|
| 7054 | Southern Rocky Mountain Ponderosa Pine Woodland |
| 7051 | Southern Rocky Mountain Dry-Mesic Montane Mixed Conifer Forest and Woodland |
| 7011 | Rocky Mountain Aspen Forest and Woodland |
| 9019 | Rocky Mountain Lower Montane-Foothill Riparian Woodland |
| 7117 | Southern Rocky Mountain Ponderosa Pine Savanna |
| 7052 | Southern Rocky Mountain Mesic Montane Mixed Conifer Forest and Woodland |
| 7107 | Rocky Mountain Gambel Oak-Mixed Montane Shrubland |
| 7049 | Rocky Mountain Foothill Limber Pine-Juniper Woodland |
| 7193 | Recently Logged-Tree Cover |
| 7061 | Inter-Mountain Basins Aspen-Mixed Conifer Forest and Woodland |
| 7016 | Colorado Plateau Pinyon-Juniper Woodland |
| 7059 | Southern Rocky Mountain Pinyon-Juniper Woodland |
| 7200 | Recently Disturbed Other-Tree Cover |
| 7385 | Great Plains Wooded Draw and Ravine Woodland |
| 7179 | Northwestern Great Plains-Black Hills Ponderosa Pine Woodland and Savanna |

*Complete treatment*

The complete treatment combining thinning and prescribed fire is assigned the same feasibility as the thinning only treatment. Although prescribed fire is not commonly used as a first-entry tool in wet forests, it is often used to manage residual surface fuels after thinning. The assumption is also that thinning makes the subsequent prescribed fire safe and limits intensity so as not to kill the remaining trees.

## Treatment cost

Treatment costs in USD $ac^{-1}$ are communicated to the model as raster surfaces. The spatial resolution and alignment of the rasters should match the LANDFIRE (2019) data used elsewhere in the WIT analyses. Treatment costs are based on local expert opinion because current treatment cost models either do not consider landscape-scale variation (Calkin and Gebert 2006) or require detailed data on stand conditions that are not available for most the landscape (Fight et al. 2006).

*Thinning*

Per acre cost for the thin only treatment is approximated as a function of base treatment cost under ideal conditions (2,500 USD $ac^{-1}$) with adjustments for distance from roads (*Dcost*) and slope steepness (*Scost*) in Eqn 1.

$$Cost = 2{,}500 + Dcost + Scost \qquad \textbf{Equation 1}$$

Cost increases with distance from roads > 800 m as specified in Eqn 2 such that the total cost of treatment increases to 10,000 USD $ac^{-1}$ at four miles from the nearest road.

$$Dcost(x) = \begin{cases} 0, & x < 800\ m \\ 1.34 * (x - 800), & x \geq 800\ m \end{cases} \quad \textbf{Equation 2}$$

Cost increases with slope > 40% as specified in Eqn 3 such that the total cost of treatment increases to 10,000 USD $ac^{-1}$ at 200% slope.

$$Scost(x) = \begin{cases} 0, & x < 40\ \% \\ 46.9 * (x - 40), & x \geq 40\ \% \end{cases} \quad \textbf{Equation 3}$$

This formulation suggests the base cost applies anywhere within 800 m of roads and less than 40% slope. Thinning cost is limited to a maximum of 10,000 USD $ac^{-1}$ when the combined distance and slope adjustments push costs above this value.

*Prescribed fire*

Prescribed fire costs are assumed to cost a uniform 1,000 USD $ac^{-1}$ based on a general estimate of planning, preparation, and implementation costs (J. White and B. Karchut, personal communication).

*Complete treatment*

Complete treatment costs are calculated as the sum of thinning and prescribed fire costs.

# Appendix III: Performance Metrics Assessment Details

## Performance metrics and descriptions

The full list of WIT performance metrics is presented in Table 14. A brief summary is provided next to explain why these metrics were calculated and what analysis methods were used (Figure 14). As a reminder, *conditional* metrics refer to the potential avoided impacts if the treated areas burn whereas *expected* metrics refer to the change in actuarial risk accounting for the likelihood of treated areas burning.

The WIT water supply risk assessment and fuel treatment optimization modules provide map, GIS, and tabular products describing some elements of the expected watershed response and impacts to water supplies but calculating these metrics for a specific project requires considerable GIS skills. The first set of metrics (Table 14) are meant to quickly summarize key watershed hazards, like total avoided hillslope erosion and sediment load to streams, and the resulting impacts to water supplies, like total avoided sediment load and sediment impact costs. These metrics are all calculated using the risk assessment framework described in Figure 2. Additionally, the analysis presents lists of downstream water infrastructure and water stakeholders (utilities). The next set of metrics (Table 14) communicate the uncertainty around the core water supply impact measures – sediment load and sediment impact costs – due to uncertainty in post-fire rainfall. Both conditional and expected measures are provided for these metrics at $5^{th}$ and $95^{th}$ percentiles of rainfall erosivity to construct an approximate 90% prediction confidence interval.

Basic descriptions of pre- and post-treatment fire behavior conditional on fire occurrence are presented next (Table 14). These measures are featured as histograms in the Peaks to People reports.

To compare the relative effectiveness and cost-effectiveness of treatment units, an estimate of treatment cost is provided based on the modeling presented in Appendix II which is used to calculate the benefit-cost ratio (BCR) of treatment by dividing the expected reduction in sediment costs to water supplies by the treatment cost. The ordered rank of treatment units based on BCR is also provided for easy identification of high priority projects.

The next section summarizes co-benefits related to wildlife and recreation (Table 14) using a simple overlay analysis to identify resources that overlap with the treatments. Avoided impacts to homes in the wildland-urban interface are summarized with both a simple count of the number of homes within 1 km of the treatment and a detailed avoided impact analysis described in the following section based on a quantitative model of home loss probability.

*Table 14: WIT performance metrics.*

| Attribute | Description |
|---|---|
| Area_ac | Fuels Reduction/Forest Restoration (acres) |
| cEro_Mg | Conditional reduction in erosion (metric tons) |
| eEro_Mg | Expected reduction in erosion (metric tons) |
| cToStrm_Mg | Conditional reduction in sediment delivered to streams (metric tons) |
| eToStrm_Mg | Expected reduction in sediment delivered to streams (metric tons) |
| cTI_Mg | Conditional reduction in sediment delivered to water supplies (metric tons) |
| eTI_Mg | Expected reduction in sediment delivered to water supplies (metric tons) |
| cTI_D | Conditional reduction in sediment costs to water supplies ($) |
| eTI_D | Expected reduction in sediment costs to water supplies ($) |
| DS_Infra | Downstream infrastructure (comma-separated list) |
| DS_Stake | Downstream stakeholders (comma-separated list) |
| cTI_Mg_05 | Conditional reduction in sediment delivered to water supplies, 5th per. rainfall (metric tons) |
| eTI_Mg_05 | Expected reduction in sediment delivered to water supplies, 5th per. rainfall (metric tons) |
| cTI_D_05 | Conditional reduction in sediment costs to water supplies, 5th per. rainfall ($) |
| eTI_D_05 | Expected reduction in sediment costs to water supplies, 5th per. rainfall ($) |
| cTI_Mg_95 | Conditional reduction in sediment delivered to water supplies, 95th per. rainfall (metric tons) |
| eTI_Mg_95 | Expected reduction in sediment delivered to water supplies, 95th per. rainfall (metric tons) |
| cTI_D_95 | Conditional reduction in sediment costs to water supplies, 95th per. rainfall ($) |
| eTI_D_95 | Expected reduction in sediment costs to water supplies, 95th per. rainfall ($) |
| Unburn_ac | Pre-treatment predicted unburned area (ac) |
| Surf_ac | Pre-treatment predicted surface fire area (ac) |
| Pass_ac | Pre-treatment predicted passive crown fire area (ac) |
| Act_ac | Pre-treatment predicted active crown fire area (ac) |
| tUnburn_ac | Post-treatment predicted unburned area (ac) |
| tSurf_ac | Post-treatment predicted surface fire area (ac) |
| tPass_ac | Post-treatment predicted passive crown fire area (ac) |
| tAct_ac | Post-treatment predicted active crown fire area (ac) |
| RedACF_ac | Active Crown Fire Reduced (ac) |
| TrtCost_D | Model estimated treatment cost ($) |
| BCR | Benefit-Cost Ratio of treatment (Risk Reduction/Treatment Cost) |
| Rank | Ordered rank of planned treatment units based on BCR |
| ParkOS_ac | Parks and open space protected from wildfire (acres) |
| WildHab_ac | Crucial wildlife habitat protected from wildfire (acres) (tiers 1 & 2 from Colorado CHAT) |
| Trail_mi | Trails protected from wildfire (miles) |
| WUI1km_n | Homes within influence zone of treatments (homes) (from Caggiano et al. 2016) |
| cHL_n | Conditional reduction in home loss (homes) |
| eHL_n | Expected reduction in home loss (homes) |
| cHL_D | Conditional reduction in home loss ($) |
| eHL_D | Expected reduction in home loss ($) |

**Home loss model**

The potential for fuel treatments to reduce structure loss is estimated using a model of home loss probability based on landscape characteristics. Price and Bradstock (2013) used multiple logistic regression to model home loss probability from structures exposed to the Black Saturday Fires in Australia and found that landscape characteristics, in contrast to fine-grained information on the home ignition zone (Cohen 2000), explained around 23% of variation in home loss. Their model predicts that the home loss increases with increasing proportion of crown fire activity and forest cover within a 1 km radius buffer around the home, the density of structures within a 50 m buffer radius around the home, and local slope. These findings are consistent with home loss studies in the US that suggest wildland urban interface disasters occur when extreme fire behavior close to a community overwhelms firefighting resources (Calkin et al. 2014) and that home loss is highest in areas of low housing density, which tend to have high proportions of natural vegetation nearby (Syphard et al. 2019). The low explanatory power of this model (r-squared = 0.23) suggests it is not appropriate for determining the fate of an individual structure. The model is instead used to estimate avoided structure loss and structure loss value across the entire analysis area assuming that the sum of marginal changes in home loss probability across many structures will result in an equivalent quantity of avoided home loss.

Individual structure locations from Caggiano et al. (2016) are used to represent building locations across the analysis area. Each structure is attributed with the median value of owner-occupied housing units by US Census tract (2015). The probability of home loss conditional on wildfire exposure is calculated per Price and Bradstock (2013) as described in equations 1 and 2 with variable definitions in Table 15.

$$x = -2.352 + 0.068(HD) + 3.697(CF) + 1.935(FA) + 0.063(S) + 1.317(HD \times CF) \quad \textbf{Equation 1}$$

$$P = \frac{e^x}{1+e^x} \quad \textbf{Equation 2}$$

Conditional home loss value is calculated as the product of the median housing value and conditional probability of loss by structure. Expected home loss and home loss value are calculated using mean burn probability calculated within a 1 km radius around each home.

*Table 15: Variable definitions, sources, and processing methods for the home loss model.*

| Variable | Definition | Source and processing |
|---|---|---|
| HD | Housing density (frequency of homes) within a 50 m radius around the target structure | Calculated with a focal neighborhood analysis of building locations from Caggiano et al. (2016) |
| CF | Proportion of area within a 1 km radius around the target structure burning as crown fire | Active crown fire from FlamMap modeling in this study |
| FA | Proportion forested within a 1 km radius around the target structure | Forest classified as ≥ 10% canopy cover from LANDFIRE (2019) |
| S | Local slope in degrees | Slope from LANDFIRE (2019) |

## Appendix IV: Installation instructions

The Watershed Investment Tool (WIT) was developed in R version 3.5.3 (R Core Team 2019). Given the nature of free and open source software to change over time, a distribution of this R version and all packages used in the WIT are provided so it will continue to function as intended into the future. No support will be provided for WIT use on other versions of R or the dependent packages. A simple graphical user interface is provided in the form of an HTML application (.hta) to allow non-technical users to progress through the scripted workflow without any knowledge of R. The graphical user interface will only work on Windows 7 and 10 operating systems. Acceptable computing performance will be achieved on machines with at least 8 GB RAM and a Core i3 processor or higher.

The WIT is distributed in zipped file folder. Unzip the contents to your preferred location on a real hard drive (e.g., the C drive on your computer, an external hard drive, or a network drive maintained by your organization). The WIT will not function properly when stored and launched from a virtual drive (e.g., Box, Dropbox, OneDrive, Google Drive, etc.). The WIT contains two HTML applications and the supporting programs and files (Figure 20). Rearranging the contents of the WIT or changing the names of the folders or files will cause it to malfunction. It is best for non-technical users to only operate the WIT through the graphical user interface (WIT.hta). This can be launched from its current location, or a shortcut can be created to launch it from the desktop or other location.

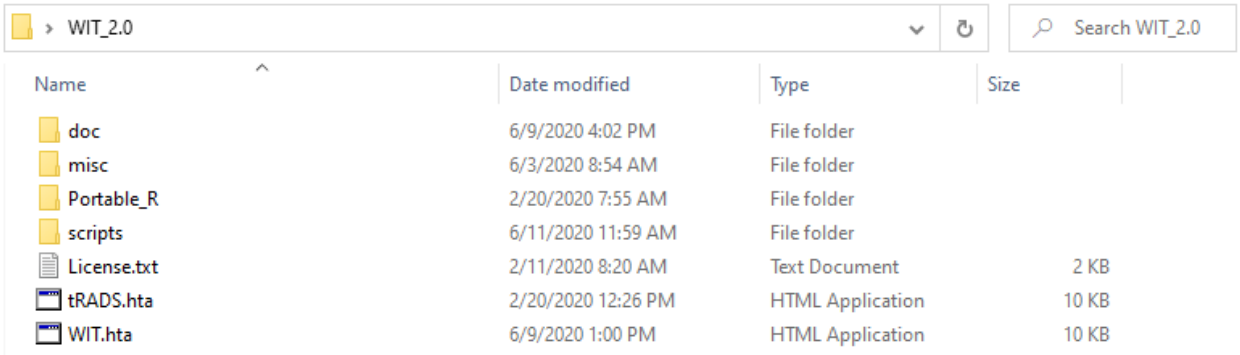


*Figure 20: Snapshot of the parent directory after unzipping. The WIT.hta is the graphical user interface. Double click to launch from this location or create a shortcut for your desktop.*

The graphical user interface (Figure 21) provides a web-like experience to progress through the sequential steps of performing a water supply risk assessment, optimizing fuel treatments to mitigate the risk, and evaluating the performance of a specific treatment plan. Inputs are flagged with green buttons and outputs are flagged with blue buttons. Grey buttons either open the reference materials provided at the top of the screen or they launch the R scripts that execute the analyses.

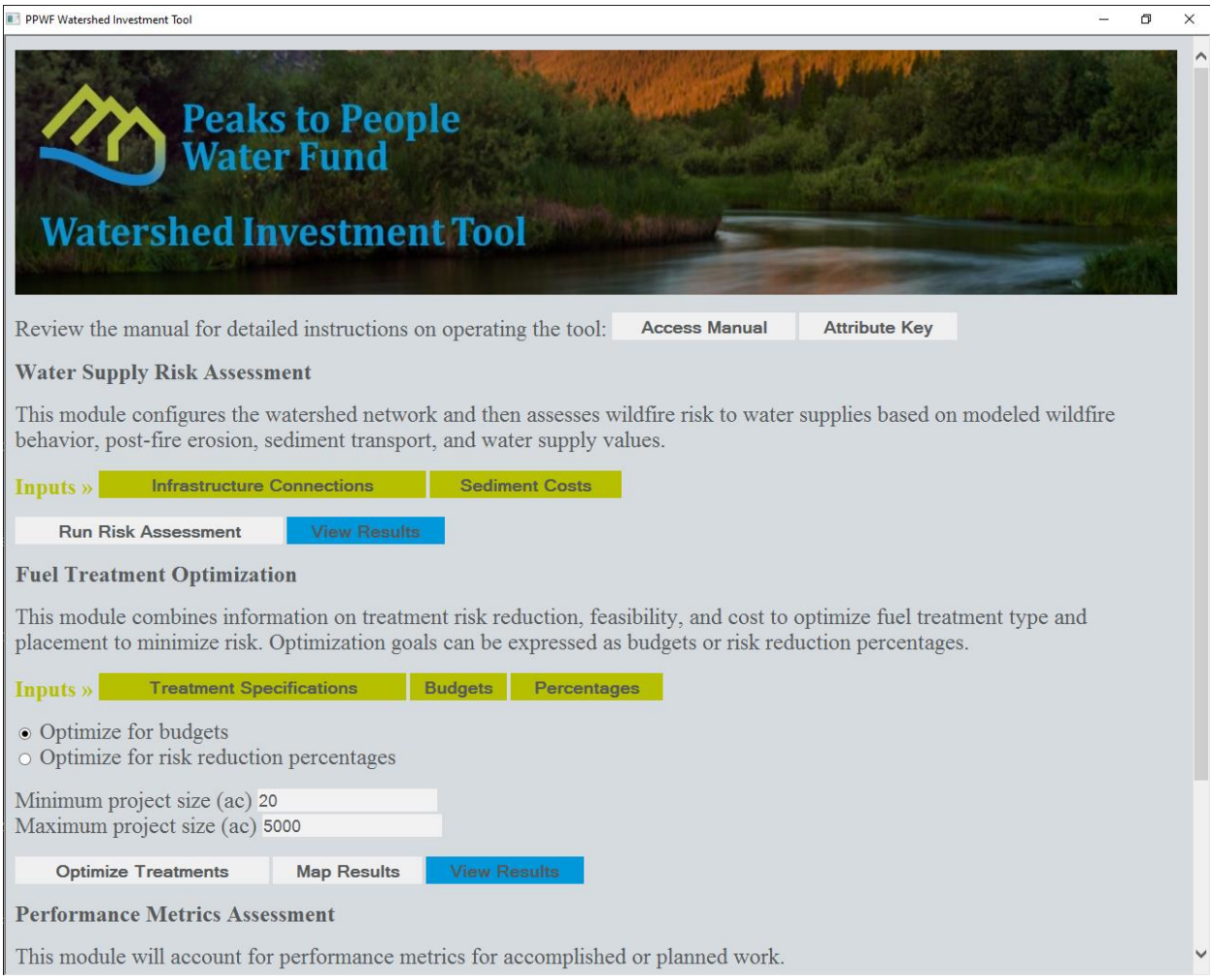


*Figure 21: Graphical user interface for the WIT.*

The WIT is preconfigured for use in the Cache la Poudre and Big Thompson Watersheds in northern Colorado. Describing all the inputs for the analysis and associated mapping is beyond the scope of this manual. All data requirements are documented within the R scripts and template directory structure housed in the scripts folder (Figure 22). Advanced users are welcome to modify data sources as they see fit to update the WIT or apply it to a different geography (see license section below). The file map (File_map.xlsx) in the *doc* folder provides a full list of files in the WIT and their functions. In addition to the WIT, several pre-processing scripts are provided (tagged with "PP") to document the fuel treatment data processing, fuelscape generation, fire modeling, and constraint modeling. This distribution of the WIT also includes the Colorado Forest Restoration Institute's Risk Assessment and Decision Support Tool (tagged with "RADS") to provide the ability to optimize risk reduction for multiple resources or assets (Gannon 2020). See the RADS manual for more details.

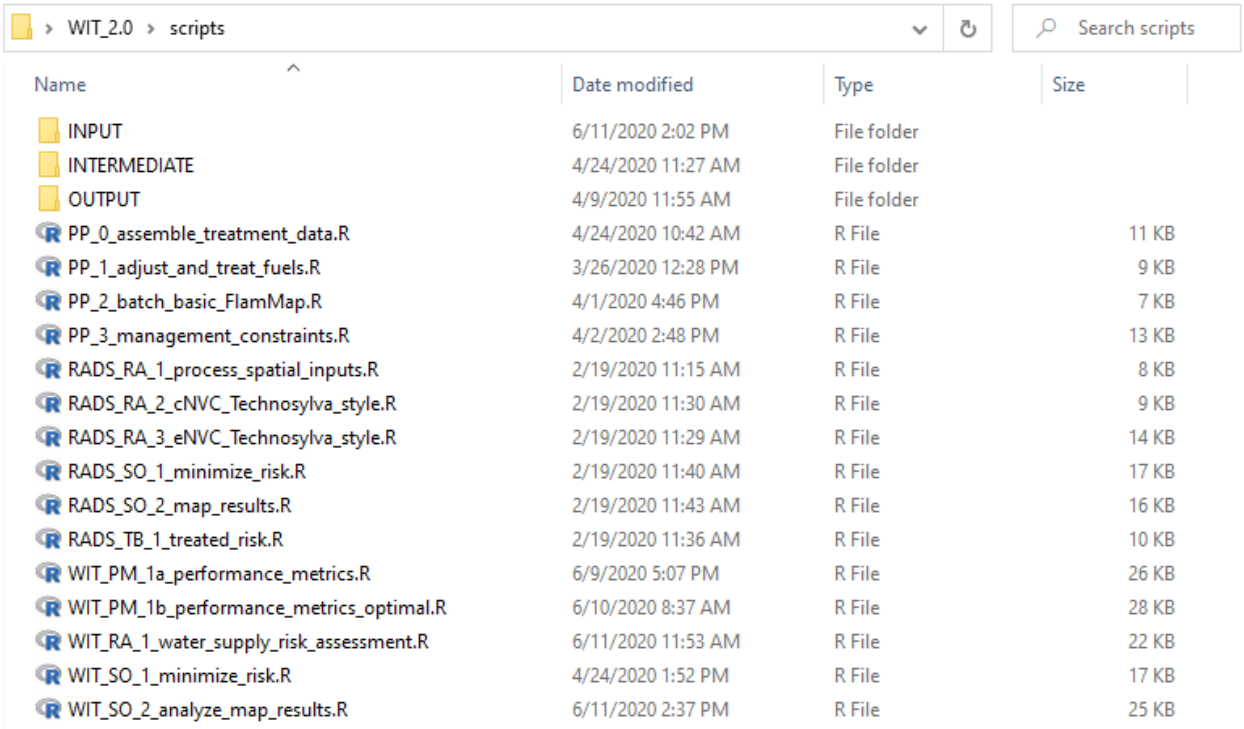


*Figure 22: Scripts folder containing the R scripts and associated directory structure for the analysis inputs and outputs.*

## License